ENERGY, EXERGY AND ECONOMIC ANALYSIS OF OFFSHORE REGASIFICATION SYSTEMS

Manuel Naveiro Parga[1,*], Manuel Romero Gómez[2], Álvaro Baaliña Insua[2], María Belén Folgueras Díaz[3]

[1] Energy Engineering Research Group, University Institute of Maritime Studies, ETSNM, University of A Coruña, A Coruña, Spain

[2] Energy Engineering Research Group, University Institute of Maritime Studies, Nautical Sciences and Marine Engineering Department, ETSNM, University of A Coruña, A Coruña, Spain

[3] Energy Department, School of Mining, Energy and Materials Engineering of Oviedo, EIMEM, University of Oviedo, Oviedo, Spain

[*] Corresponding author.

Correspondence

Manuel Naveiro, Energy Engineering Research Group, University Institute of Maritime Studies, ETSNM, University of A Coruña, Paseo de Ronda 51, A Coruña 15011, Spain
E-mail: manuel.naveiro@udc.es

ABSTRACT

An energy, exergy and economic analysis is proposed herein to evaluate regasification systems in Floating Storage Regasification Units (FSRUs). Three regasification systems typical in these types of vessels are considered: seawater system, open loop propane system and closed loop water-glycol system. The energy and exergy analyses were performed using the Engineering Equation Solver (EES), while Suite AspenONE programs were used for the economic assessment. The exergy analysis provides a better

understanding of the components of physical exergy (thermal and mechanical exergy) in order to define an exergy efficiency applicable to any liquefied natural gas (LNG) regasification system or FSRU. The results obtained prove the seawater regasification system to be most efficient from an energy and exergy standpoint. The specific energy consumption and exergy efficiency for this system are 227.33 kJ/kg and 50.00 %, respectively. On the other hand, the open loop propane regasification system is most cost-effective for an LNG price between 1.32 and 11 USD/MMBtu. The vast amounts of destroyed exergy in the regasification process of current systems was also demonstrated and hence the need to develop new, more efficient configurations that could exploit the cold energy of LNG.

Keywords

cold energy, economic analysis, exergy efficiency, floating storage regasification unit, liquefied natural gas regasification

Nomenclature

Symbols

A	area (m^2)
b	specific consumption (kJ/kg) or (kJ/kW-h)
$\dot{C}, \dot{Z}$	cost rate (USD/min)
d	diameter (mm)
$\dot{E}$	exergy flow rate (kW)
e	specific flow exergy (kJ/kg)
$\dot{H}$	energy flow rate (kW)
h	enthalpy (kJ/kg) or film heat transfer coefficient (W/m^2-K)
$\dot{I}$	irreversibilities (kW)
k	conductivity (W/m-K)
L	longitude (m)
$\dot{m}$	mass flow rate (kg/s)
n	moles (-) or lifetime (years)
NTU	number of transfer units
Nu	Nusselt number (-)
p	pressure (bar)
p_t	pitch (mm)
$\dot{Q}$	heat transfer rate (kW)
Re	Reynolds number (-)
R_f	fouling resistance (m^2K/W)
s	entropy (kJ/kg-K)
T	temperature (ºC)
U	overall heat transfer coefficient (W/m^2-K)
$\dot{W}$	power (kW)

y	mole fraction (-)
β_{CRF}	capital recovery factor (-)
γ_{OM}	operation and maintenance factor (-)
ε	effectiveness (-)
η	efficiency (-)
τ	annual operating hours (h)
φ	chemical exergy factor for fuels (kJ/kg)

Subscripts and Superscripts

0	reference condition
alt	alternator
b	baseline or boiler
ch	chemical
CI	capital investment
comb	combustion
CSW	cooling seawater
ec	economizer
el	electric
eng	engine
ex	exergy
f	fuel
FW	freshwater
g	gases
i	inlet, interest, internal
l	liquid water
LHV	lower heating value
n	natural
o	output, external
OM	operation and maintenance
p	pressure, products
ph	physical
r	reactants
s	shell
SW	seawater
t	tube
th	thermal
tk	storage tank
tot	total
w	wall

Abbreviations

3E	energy, exergy, economic
AC/NGH	after cooler/natural gas heater
BOG	boil off gas
BOR	boil off rate
CEPCI	Chemical Engineering Plant Cost Index
CP	centrifugal pump
DC	drain cooler (condenser)
DFDE	dual fuel diesel electric
DO	diesel oil
E	economizer
EES	Engineering Equation Solver
FCI	fixed capital investment
FSRU	floating storage regasification unit
FV	forcing vaporizer
GCU	gas combustion unit
LD	compressor low duty
LNG	liquefied natural gas
MX	mixer
NG	natural gas
ORC	organic Rankine cycle
P	pump
PE	propane evaporator
PH	preheater
PHE	plate heat exchanger
R	recondenser
RS	regasification system
S	separator
S&T	shell and tubes heat exchanger
TH	trim heater
VP	LNG vaporizer
WGH	water-glycol heater

1 Introduction

Liquefied natural gas (LNG) comprises a mixture of light hydrocarbons together with nitrogen that is liquefied in export terminals, also termed liquefaction plants, for its subsequent storage in tanks at a temperature of approximately -162 ºC and at a pressure slightly above atmospheric [1]. Natural gas stored in the liquid state is sea transported by LNG carriers to the regasification terminals. In these, natural gas is returned in supercritical conditions to the gas pipeline network for its distribution and commercialization. Regasification can be performed in both onshore or offshore terminals, as is the case with Floating Storage and Regasification Units (FSRUs) [2].

FSRUs are not considered a substitute for onshore terminals, but rather a supplement. That is, there are circumstances in certain projects that favour the installation of the former [3]. Some of these factors are due to political, economic, or location, planning and public safety-related reasons, or also because of environmental limitations.

Since 2005, the year in which the first offshore regasification terminal was inaugurated in the Gulf of Mexico [4], until late 2019, a total of 35 regasification vessels were built [5]. Most of the new build FSRUs are usually fitted with membrane tanks developed by Gaztransport & Technigaz (NO 96, MARK III, ...) for LNG storage and an electric propulsion system with alternators powered by dual fuel (DF) engines, capable of operating with different fuels: diesel oil, fuel oil and natural gas. This propulsion system is termed dual fuel diesel electric (DFDE).

Regasification systems installed on FSRUs can be classified according to the heat source (open, closed or combined loop) and the method in which the heat exchange takes place between the source and the LNG (direct or indirect). Open loop uses seawater at room temperature, while the closed loop employs the energy released in combustion processes, most often the steam produced in boilers. The combined loop entails both heat sources and is often used in cases where the seawater temperature is slightly below the design minimum [6]. The regasification system is considered indirect if there is an intermediate fluid operating in a closed circuit in the heat exchange process, between the source and the LNG.

The choice of the type of work loop must have the approval of the authority**.** As a general rule, the open loop is normally approved, provided that the seawater discharge temperature is not excessively cold. However, it has been prohibited in countries such as the United States due to the physical and chemical damage caused by the consumption and continuous discharge of seawater on marine organisms [7]. Closed loop regasification systems comply with the most stringent conditions regarding the protection of the marine environment [8] but fuel consumption and, consequently, flue gas and particulate emissions are higher when compared with open loop systems. Therefore, most FSRUs usually have a regasification system that can operate in open loop [9]. Such systems

typically employ seawater in direct exchange or propane as an intermediate fluid, although the latest regasification systems substitute propane for a water-glycol solution [10], which was previously used in FSRUs that operated exclusively in a closed loop.

In any case, regasification systems installed to date in FSRUs do not exploit the LNG cold energy potential effectively. However, companies in the sector have demonstrated interest in applying proven technologies of onshore terminals that can reduce fuel consumption and improve FSRU efficiency during the regasification process [11]. On this point, Tianbiao et al. [12] consider power generation to be the main usage of LNG cold energy in FSRUs. However, they also mention the limited deck space and the need to design compact units as key to their effective implementation. Furthermore, in order to propose more efficient regasification systems, the economic assessment should not be ignored [13].

The energy, exergy and economic (3E) analysis offer the advantage of evaluating systems and equipment and the effect of significant parameters on them from the thermodynamic and economic point of view. Furthermore, this type of analysis is suitable when dealing with multi-objective optimization problems, where, in addition to minimizing the total cost (investment, operation and maintenance), other aspects (efficiencies, environmental, ...) are taken into consideration. The 3E analysis has been widely implemented in the assessment of thermodynamic cycles to recover the LNG cold energy [13]. However, few studies evaluate the prospects for exploiting LNG cold energy on board ships [14]. Within this reduced number of publications, even fewer include a thermo-economic analysis. These studies focus on the installation of organic Rankine cycles (ORC) on LNG-fuelled vessels that use the high temperature waste heat energies of DF engines as heat sources and the cryogenic temperature of LNG as a sink. Tsougranis and Wu [15] analysed the energy, exergy and economic feasibilities of installing a regenerative ORC and a reheat regenerative ORC with direction expansion of the natural gas on board a passenger vessel. The thermal efficiency estimate for the two cases are 28.4 and 35.7 %, respectively. Han et al. [16] propose a triple ORC for LNG fuelled-vessels optimized with 15 optional working fluids. The multi-objective self-adaptative firefly algorithm is used to optimize the waste energy utilisation rate and the cost productivity functions of the system. Koo et al. [17] evaluate and optimise the exergy efficiency and the actual annualized cost for six ORC architectures (three for high pressure DF engines and three for low pressure DF engines). Tian et al. [18] perform thermo-economic analysis and multi-objective optimization of a combined ORC system with LNG cold energy and DF marine engine waste heat utilization. The study evaluates 32 working fluids and employs thermal efficiency and economic index as objective functions. The combinations R1150-R600a-R290, R1150-R601a-R600a and R170-R601-R290 give the best results. Despite the potential benefits of exploiting cold energy in LNG-fuelled vessels studied by the above papers, these are dwarfed when compared to the high flow of natural gas discharged to shore by the regasification system of the FSRUs.

Literature that addresses the thermodynamic and thermo-economic analyses of regasification systems in FSRUs is scarce, focusing on the study of open loop systems that incorporate the ORC technology. Yoon-Ho [19], based on studies of Yao et al. [20] and Lee et al. [21], performs the thermo-economic analysis of a simple ORC (1-ORC) and a two-stage ORC in series (2-ORC) with zeotropic mixtures of ethane and propane. The 2-ORC with pure propane in the high-temperature cycle and an 8:2 ethane/propane mixture in the low-temperature cycle obtains the best results, increasing energy and exergy efficiencies by 75 % compared to the 1-ORC with a 6:4 ethane/propane mixture. In another publication, Yoon-Ho [22] performs a thermo-economic analysis of six configurations with pure working fluids: 1-ORC with propane; 2-ORC with propane and ethane; three-stage ORC in series (3-ORC) with propane, ethane and butane; and the corresponding versions of each cycle in combination with a regasified NG expander, which only expands the NG flow consumed by the engines. In this case, the 3-ORC with partial expander improves the energy and exergy efficiency by 2.3 times compared to 1-ORC with propane. To achieve higher exergy efficiency, Yao et al. [23] propose cascade three-level ORCs as an alternative to ORCs in series.

No previous publication deals with the analysis of closed loop regasification systems, which, despite a higher fuel consumption, are beneficial in terms of environmental burden as these do not involve the continuous pumping of seawater. Moreover, although there are studies that evaluate the irreversibility of the different components, none define an exergy efficiency that includes the very efficiency of the regasification process, nor does any determine the global efficiency of the regasification vessel Therefore, the development of a new exergy analysis method to determine the rational efficiency of the regasification process is essential. This implies an in-depth study of the physical exergy terms of natural gas, as regasification is initially a dissipative process where exergy balance cannot be applied with conventional terms to properly define the exergy efficiency.

The objective of this study is to establish the bases of the 3E analysis, including the novel approach of exergy efficiency calculation, that allow the assessment and comparison of both current and future regasification systems, whether they have methods that exploit the LNG cold energy in place or not. For this purpose, the present paper examines three typical regasification systems: seawater system, open loop propane system, and closed loop water-glycol system. The energy and exergy analyses are carried out with Engineering Equation Solver (EES) software, while the AspenONE Suite programs are used for the economic assessment.

2 Systems description and assumptions

The characteristics of the model FSRU, the description of the regasification systems and the assumed parameters used for the analysis are presented below in sections 2.1, 2.2 and 2.3, respectively.

2.1 FSRU characteristics

Prior to the analysis of the regasification systems, the basic FSRU model characteristics are defined taking recent constructions into account:

- Mark III tanks with a maximum vapour pressure of 0.7 bar gauge and a boil off rate (BOR) of 0.15 % [24].
- Cargo capacity of 170 000 m^3 [5].
- Two-stage low duty (LD) compressors with pre-cooling by spraying the LNG supplied by the gas fuel pump.
- After cooler/natural gas heater (AC/NGH) with fresh water cooling.
- Forcing vaporizer (FV) with auxiliary system steam.
- Maximum natural gas flow of 750 mmscfd; equivalent to 3 regasification modules in operation [9].
- DFDE propulsion with 3 Wärtsilä 12V50DF (11.4 MW) and 1 Wärtsilä 6L50DF (5.7 MW).
- Economizer for each of the internal combustion engines.

Specific energy consumption of the engines and AC/NGH characteristics are presented in Table 1 and Table 2. Data were collected from a current LNG vessel.

Table 1
Specific energy consumption of 50DF engines.

Load (%)	**Specific energy consumption (kJ/kW-h)**	
	Natural gas	**Pilot DO**
25	11 922.7	234.4
50	9286.7	77.2
75	8258.4	30.1
100	7665.4	19.2

Table 2
AC/NGH design data.

Component	Parameter	Value
Tubes	Tubes per pass	100
	Passes	2
	Pattern	Square
	External diameter (mm)	15.875
	Thickness (mm)	0.889
	Pitch (mm)	21
	Length (mm)	2500
	Material	SS304L
Shell	Passes	1
	External diameter (mm)	414
	Thickness (mm)	7
Baffles	Number	8
	Space between baffles (mm)	250
	Baffle cut (%)	25

2.2 Regasification systems

Regasification systems are simplified for analysis. The LNG regasification process for each of these is described below.

The seawater regasification system studied, similar to that proposed by some companies [25] is depicted in Figure 1. The low pressure pump (primary or feed) supplies the LNG (1-2) stored in the tank to the recondenser (R), after having passed through the corresponding valve. It is considered that the LNG pressure drops prior to the recondenser inlet (2-3) take place in that valve. The LNG extracted from the recondenser is driven by the high pressure pump (secondary or booster) (4-5) towards the vaporizer fed with seawater (VP). The LNG is heated up to the natural gas (NG) distribution temperature (6) in the vaporizer by means of the seawater (16) supplied by the corresponding pump. The boil off gas (BOG) (10) is cooled to a temperature of -120 ºC, spraying the LNG (8) supplied by the fuel gas pump in the mixer (MX). Once the condensables are removed in the separator (S), the BOG is driven by the LD compressor (11-12) towards the AC/NGH and the recondenser. Should the BOG generated in the tanks be insufficient to maintain a constant pressure therein, the LNG is vaporized with the FV, which has a control system to maintain the temperature at the outlet at -120 ºC (9). The BOG consumed by the engines is conditioned in the AC/NGH (12-14). The remaining BOG passes through the corresponding valve, causing the pressure drops up to the recondenser inlet (12-13). The BOG is condensed in the recondenser and mixed with the LNG supplied by the primary pump. If the BOG generated in the tanks cannot be managed, it is sent to the Gas Combustion Unit (GCU).

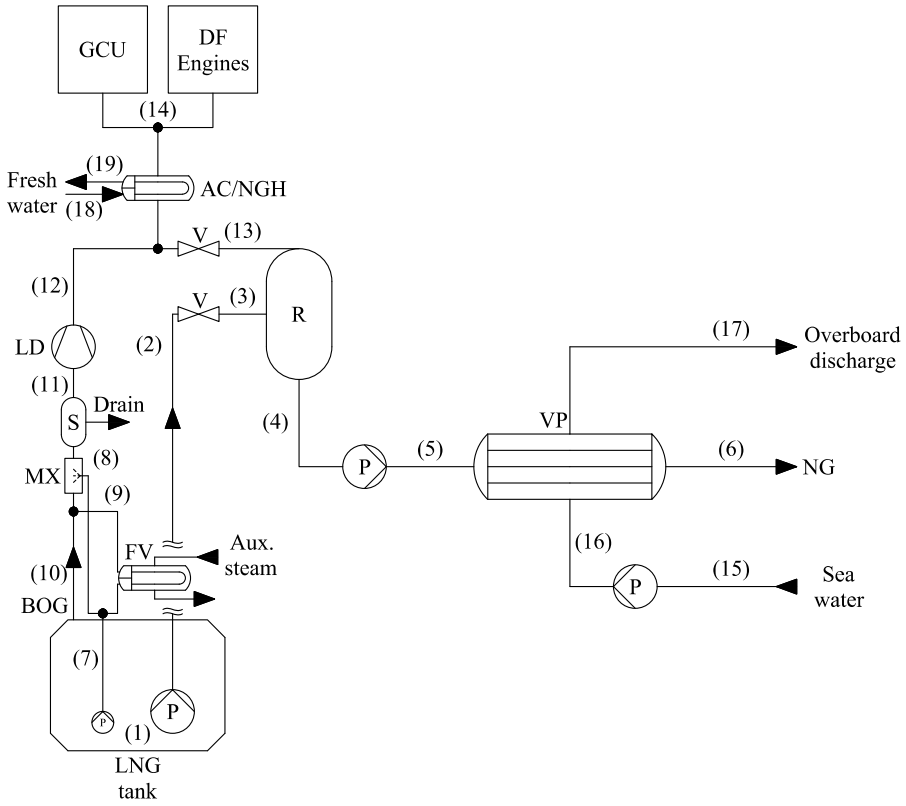

Figure 1. Schematic diagram of the seawater regasification system.

Figure 2 below illustrates the open loop propane regasification system analysed, similar to that installed in some FSRUs [26]. The configuration is practically identical to the seawater regasification system except it includes the propane intermediate circuit. Propane leaves the LNG vaporizer (VP) in subcooled liquid conditions (16) and is then driven by the pump (16-17) towards the propane evaporator (PE) inlet, from where it leaves in wet vapour conditions (18). The propane then returns to the LNG vaporizer, thereby closing the cyclical process. The seawater is driven by the pump (19-20) towards the propane evaporator and the trim heater (TH).

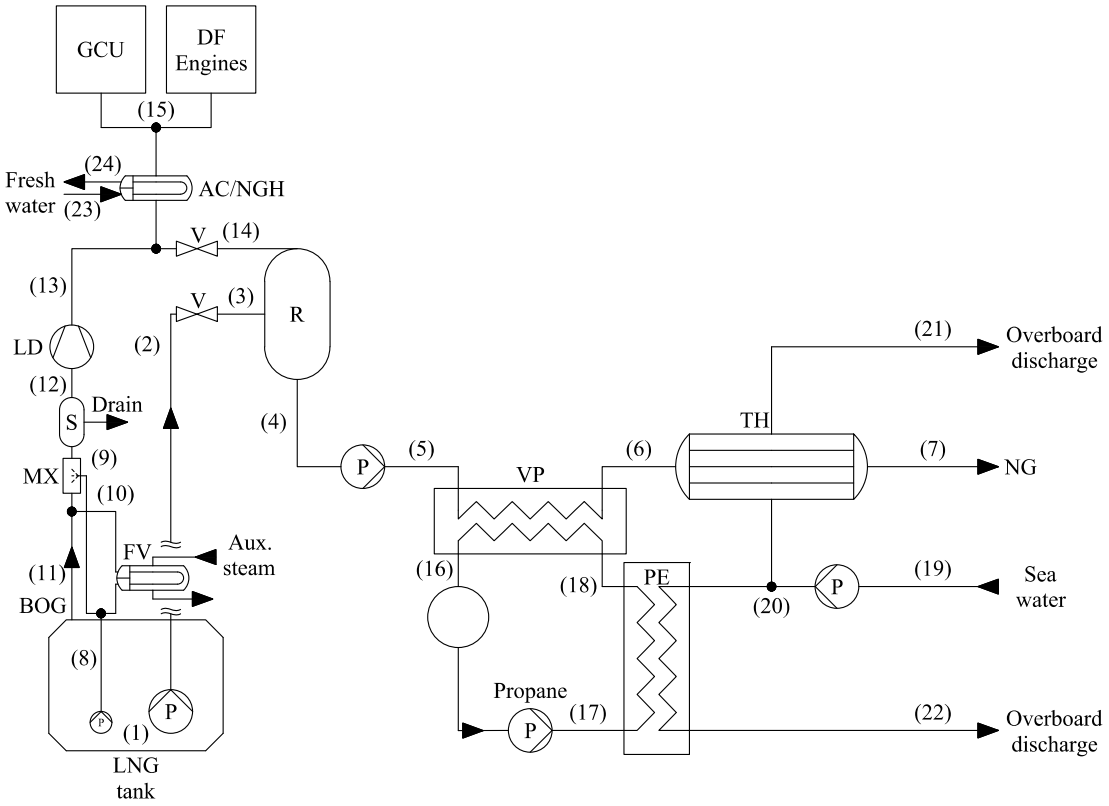

Figure 2. Schematic diagram of the open loop propane regasification system.

Lastly, the analysed closed loop water-glycol regasification system is shown in Figure 3, which is similar to those installed in some regasification vessels [27]. The water-glycol mixture lowers its temperature in the LNG vaporizer (19-17) and is subsequently driven by the pump (17-18) towards the heater (WGH) inlet. The mixture (19), at a temperature of 90 ºC, leaves the heater and returns to the vaporizer, thereby closing the cyclical process. On the other hand, the water of the feed tank (FT) is supplied by the corresponding pump (20-21) towards the preheater (PH), in which the fluid temperature is increased to 135 ºC (22). The water then circulates through the economizer and enters the steam drum. From here the fluid descends through the downcomers towards the water drum. The water deriving from here is partially vaporized in the tube bank, returning in wet steam conditions to the steam drum. The saturated steam is extracted from the upper part of the steam drum (24). The steam produced by the boiler is split into two heating circuits depending on its pressure. High pressure steam (25) is used in the water-glycol heater and returns to the feed tank in liquid state (27). However, the low pressure steam (28 and 31) is used to increase the temperature of the water in the preheater and feed tank. The water (30 and 33) circulating through the preheater traps (T) and feed tank coil is subcooled (34) in the condenser/drain cooler (DC), returning to the feed tank. With regard to the boiler combustion process, the BOG consumed (16) reacts with the air driven by the forced draft fan (FDF) (35-36). The flue gases (37) enter the economizer, decrease in

temperature (38), and increase the temperature of the water (23) to a value close to that of saturated liquid.

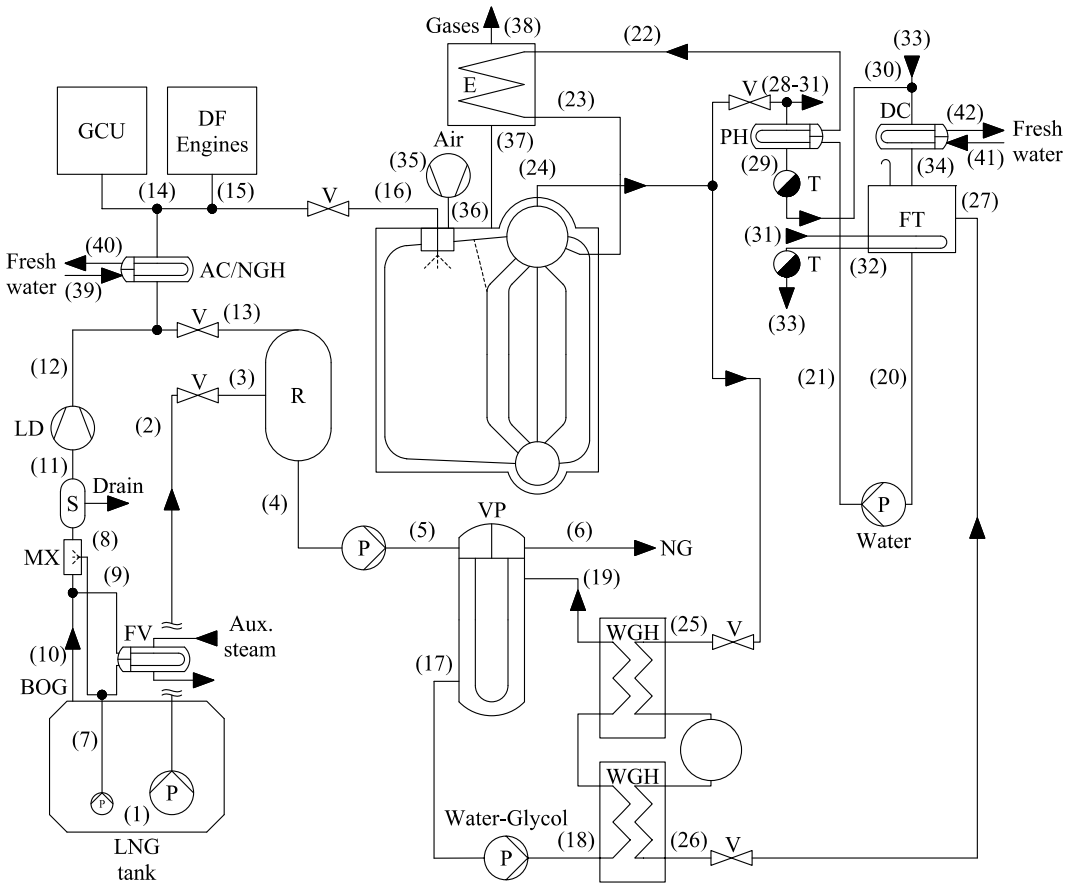

Figure 3. Schematic diagram of the closed loop water-glycol regasification system.

2.3 Assumptions

The following general conditions are established for the study of regasification systems:

- Reference state of 25 ºC and 1 atm [28] for calculating the exergy.
- Steady state in all processes, except for the cargo tank mass balance.
- Effects associated with kinetic and potential energy are neglected.
- Natural gas composed solely of methane.
- Natural gas flow of 500 mmscfd (60 ºF and 1 atm), which is equivalent to two regasification modules in operation and another in stand-by (baseload regasification capacity) [8].
- Equipment in adiabatic conditions, except for cargo tanks.
- In the economizers, engines exhaust gases produce 100 % of the heat output required in the auxiliary steam system.
- Minimum temperature difference in heat exchange processes of 5 ºC.
- Cargo tanks with a balanced two-phase liquid-vapour mixture. That is, homogeneous temperature and pressure. The mathematical model is explained in section 3.1.
- AC/NGH based on the data in Table 2 using the ε-NTU method. The Gnielinski correlation is employed in the film coefficient calculation of the fluid that circulates inside the tubes [29], while the approximate Bell-Delaware method is applied to the fluid that flows through the shell [30]. Section 3.2 provides the validation of the heat transfer model with real data for different cases.
- Table 3 contains the general conditions in the analysis of regasification systems [25–27].

Table 3
General conditions of regasification systems.

Parameter	**Value**
LNG tank pressure	1.16325 bar
BOG temperature before the mixer (pre-cooling)	-100 ºC
Natural gas mass flow rate	111.19 kg/s
Regasified natural gas pressure	85 bar
Regasified natural gas temperature	10 ºC
Natural gas lower heating value	49 500 kJ/kg
DO lower heating value	42 700 kJ/kg
Baseline electricity consumption	2050.9 kW
Alternator efficiency	95 %
Pumps isentropic efficiency	80 %
Pumps electromechanical efficiency	90 %
Feed pump discharge pressure	9 bar
Booster pump discharge pressure	110 bar
LD isentropic efficiency	55 %
LD electromechanical efficiency	80 %
BOG temperature after the mixer (pre-cooling)	-120 ºC
LD discharge pressure	6 bar
Recondenser pressure	5.5 bar
BOG pressure loss through the AC/NGH	0.1 bar
Fresh water flow rate through the AC/NGH	30 000 kg/h
Fresh water pressure loss through the AC/NGH	2.5 bar
Fresh water pressure loss through the AC/NGH	0.15 bar
Fresh water temperature at the AC/NGH inlet	36 ºC

The following specific conditions are included in the analysis of open loop regasification systems:

- Sea water temperature of 15 ºC for regasification systems, usually considered as the minimum possible under design conditions. Salinity of 35 g/kg. The seawater library of EES is used to calculate its properties [31,32].
- Maximum variation in seawater temperature between inlet and outlet of 5 ºC.
- Sea water pump discharge pressure of 7.5 bar.
- Seawater circuit pressure loss focused on the heat exchange processes.
- Table 4 lists the specific conditions of the propane regasification system [26].

Table 4
Open loop propane regasification system conditions.

Parameter	**Value**
Natural gas pressure loss through the vaporizer	23 bar
Natural gas temperature at the vaporizer outlet	-20 ºC
Propane pump suction pressure	3.5 bar
Propane pump discharge pressure	6 bar
Propane pressure at the vaporizer inlet	5.5 bar
Propane vapour quality at the vaporizer inlet	0.8
Propane temperature at the vaporizer outlet	-15 ºC

Lastly, the following is established for the analysis of the water-glycol regasification system:

- Concentration of ethylene glycol in the water on a mass basis of 30 %**.** The water-glycol mixture is modelled as an incompressible fluid.
- Molar composition of air in the boiler combustion process of 21 % oxygen and 79 % nitrogen. The ideal gas model is implemented.
- State of saturated liquid at the steam trap inlet and isenthalpic expansion up to condenser pressure.
- Temperature and pressure of the cooling water at the condenser inlet identical to that of the AC/NGH.
- Table 5 groups the particular conditions of the water-glycol regasification system [27].

Table 5
Closed loop water-glycol regasification system conditions.

Parameter	**Value**
FDF electromechanical efficiency	90 %
FDF isentropic efficiency	80 %
Flue gas pressure loss through the boiler	0.05 bar
Combustion efficiency (boiler)	97 %
Boiler efficiency	90 %
Excess air	10 %
Water-glycol pump suction pressure	3.5 bar
Water-glycol pump discharge pressure	6 bar
Water-glycol pressure at the vaporizer inlet	5.5 bar
Water-glycol temperature at the vaporizer inlet	90 ºC
Water pressure at the feed tank	1.01325 bar
Water temperature at the feed tank	90 ºC
Water temperature at the pre-heater outlet	135 ºC
Approach temperature (economizer)	5 ºC
Saturation pressure at steam dome	29 bar
Steam pressure at the water-glycol heater inlet	25.5 bar
Water pressure at the water-glycol heater outlet	2.5 bar
Water temperature at the water-glycol heater outlet	25 ºC
Heating steam pressure	9 bar
Water temperature at the condenser outlet	90 ºC
Fresh water temperature at the condenser outlet	44 ºC

3 Mathematical modelling

The equations used to perform the 3E analysis of the regasification systems are presented below. Section 3.1 describes the BOG generation model in the LNG storage tanks, section 3.2 presents the heat transfer model of the AC/NGH, section 3.3 details the analysis based on the first law of thermodynamics, section 3.4 introduces the exergy balance of each component and the novel concept of exergy efficiency, and section 3.5 describes the economic method implemented.

3.1 BOG generation in LNG storage tanks

The BOG generated in the storage tank ($\dot{m}_{\mathrm{BOG}}$) is calculated by applying the mass balance in non-stationary processes:

$$\frac{dm_{\mathrm{tk}}}{dt} = -\left(\dot{m}_{\mathrm{BOG}} + \dot{m}_{\mathrm{LNG,t}}\right) \tag{1}$$

where the mass change per unit of time in the control volume ($\frac{dm_{\mathrm{tk}}}{dt}$) is equal to the combined mass flow of BOG and extracted LNG ($\dot{m}_{\mathrm{LNG,t}}$).

The LNG extracted from the tank is the sum of the mass flows driven by the feed pump ($\dot{m}_{\mathrm{LNG}}$) and the fuel gas pump ($\dot{m}_{\mathrm{LNG,fg}}$):

$$\dot{m}_{\mathrm{LNG,t}} = \dot{m}_{\mathrm{LNG}} + \dot{m}_{\mathrm{LNG,fg}} \tag{2}$$

Eq. (1) is equivalent to the following system of equations:

$$\frac{dm_{\mathrm{tk}}}{dt} = \frac{dm_{\mathrm{tk,LNG}}}{dt} + \frac{dm_{\mathrm{tk,BOG}}}{dt} \tag{3}$$

$$\frac{dm_{\mathrm{tk,LNG}}}{dt} = -\left(\dot{m}_{\mathrm{LNG,t}} + \dot{m}_{\mathrm{BOG,n}}\right) \tag{4}$$

$$\frac{dm_{\mathrm{tk,BOG}}}{dt} = \dot{m}_{\mathrm{BOG,n}} - \dot{m}_{\mathrm{BOG}} \tag{5}$$

in which the tank has been divided in the vapour and liquid zone.

The natural BOG mass flow ($\dot{m}_{\mathrm{BOG,n}}$) is defined as [33]:

$$\dot{m}_{\mathrm{BOG,n}} = BOR\, V_{\mathrm{tk}}\, \rho_{\mathrm{LNG}} \tag{6}$$

where BOR is the boil-off rate, V_{tk} is the total load volume and ρ_{LNG} the LNG density.

The total volume of the tank remains unchanged, therefore, it is fulfilled that the variation of the volume in the liquid zone ($\frac{dV_{\mathrm{tk,LNG}}}{dt}$) plus that of vapour ($\frac{dV_{\mathrm{tk,BOG}}}{dt}$) equals zero [34]:

$$\frac{dV_{\mathrm{tk,LNG}}}{dt} + \frac{dV_{\mathrm{tk,BOG}}}{dt} = 0 \tag{7}$$

On the other hand, $\frac{dV_{\mathrm{tk,LNG}}}{dt}$ is:

$$\frac{dV_{\mathrm{tk,LNG}}}{dt} = -v_{\mathrm{LNG}}\left(\dot{m}_{\mathrm{LNG,t}} + \dot{m}_{\mathrm{BOG,n}}\right) \tag{8}$$

Furthermore, $\frac{dV_{\mathrm{tk,BOG}}}{dt}$ is related with $\frac{dm_{\mathrm{tk,BOG}}}{dt}$ through the specific volume in the vapour zone (v_{BOG}):

$$\frac{dV_{\mathrm{tk,BOG}}}{dt} = v_{\mathrm{BOG}}\frac{dm_{\mathrm{tk,BOG}}}{dt} \tag{9}$$

Combining Eqs. (5), (7), (8) and (9) yields:

$$\dot{m}_{\mathrm{BOG}} = \dot{m}_{\mathrm{BOG,n}} - \frac{v_{\mathrm{LNG}}}{v_{\mathrm{BOG}}}\left(\dot{m}_{\mathrm{LNG,t}} + \dot{m}_{\mathrm{BOG,n}}\right) \tag{10}$$

The BOG available on the vessel is calculated by solving Eqs. (2), (6) and (10).

3.2 AC/NGH heat transfer model

The AC/NGH mathematical model developed involves the application of the energy balance in combination with the ε-NTU exchanger design method and the calculation of the overall heat transfer coefficient. Pressure drops are considered constant.

The overall external heat transfer coefficient (U_{o}) can be expressed as:

$$U_{\mathrm{o}} = \frac{1}{\frac{1}{h_{\mathrm{s}}} + R_{\mathrm{f,s}} + \frac{d_{\mathrm{o}} \ln\left(\frac{d_{\mathrm{o}}}{d_{\mathrm{i}}}\right)}{2k_{\mathrm{w}}} + \left(\frac{d_{\mathrm{o}}}{d_{\mathrm{i}}}\right)\left(\frac{1}{h_{\mathrm{t}}} + R_{\mathrm{f,t}}\right)} \tag{11}$$

where h_{s} and h_{t} are the film coefficients of the fluids circulating through the shell and the tubes, $R_{\mathrm{f,s}}$ and $R_{\mathrm{f,t}}$ are the fouling resistances of both fluids, d_{i} is the internal diameter of the tubes and k_{w} is the thermal conductivity of their material.

The convection coefficient of the shell is calculated by applying the Bell Delaware method, the general equation being:

$$h_{\mathrm{s}} = h_{\mathrm{id}} J \tag{12}$$

where h_{id} is the ideal convection coefficient in a tube bank with cross flow and J represents the product of the correction factors of the various flows in the exchanger whose value approaches 0.60 [30].

The correlations used to calculate the Nusselt number and the friction factor correspond to those included in EES for turbulent flows inside tubes [29]. Therefore, the Gnielinski correlation is applied along with the entrance correction factor.

Validation of the AC/NGH mathematical model is performed by comparing the results obtained in the EES with the reference values of the parameters to be calculated, the temperatures of the fluids at the exchanger outlet and the heat flow rate, for each of the six cases included in Table 6. The maximum percentage error is associated with the BOG temperature at the exchanger outlet (case 4), which reaches 4.22 %. However, the percentage errors in the exchanged heat flow rate and in the water temperature at the AC/NGH outlet are under 2.63 % (case 1) and 0.15 % (case 4), respectively. Therefore, the implemented mathematical model is considered adequate.

Table 6
Comparison between the results obtained from the mathematical model and the reference values of the AC/NGH for various cases.

		Case					
		1	**2**	**3**	**4**	**5**	**6**
Shell (methane)							
Mass flow rate (kg/h)		6142	5469	4990	6321	5669	2103
Inlet temperature (ºC)		13.00	12.70	17.80	4,40	12.80	39.00
Inlet pressure (bar)		6.50	6.50	6.50	6.50	6.50	6.50
Outlet temperature (ºC)	Reference	33.20	33.50	34.20	32.00	33.40	36.10
	Model	32.24	32.64	33.64	30.65	32.52	36.12
	Error (%)	2.89	2.57	1.64	4.22	2.63	0.06
Heat flow rate (kW)	Reference	76	69	50	106	71	4
	Model	74	68	50	104	70	4
	Error (%)	2.63	1.45	0.00	1.89	1.41	0.00
Tubes (water)							
Mass flow rate (t/h)		30	30	30	30	30	30
Inlet temperature (ºC)		36.00	36.00	36.00	36.00	36.00	36.00
Inlet pressure (bar)		2.50	2.50	2.50	2.50	2.50	2.50
Outlet temperature (ºC)	Reference	33.83	34.01	34.56	32.97	33.95	36.11
	Model	33.87	34.03	34.57	33.02	33.98	36.11
	Error (%)	0.12	0.06	0.03	0.15	0.09	0.00

3.3 Energy analysis

Regasification systems were analysed with EES software using the first and second laws of thermodynamics. For pumps and compressors, the power ($\dot{W}$) and isentropic efficiency (η_s) were defined respectively as:

$$\dot{W} = \dot{m}(h_o - h_i) \tag{13}$$

and

$$\eta_s = \frac{h_{o,s} - h_i}{h_o - h_i} \tag{14}$$

where $\dot{m}$ is the mass flow through the unit, $h_o - h_i$ is the actual enthalpy change and $h_{o,s} - h_i$ is the enthalpy change under isentropic conditions. The electrical power ($\dot{W}_{\mathrm{el}}$) consumed by these components can be calculated using Eq. (15):

$$\dot{W}_{\mathrm{el}} = \frac{\dot{W}}{\eta_{\mathrm{el,m}}} \tag{15}$$

where $\eta_{\mathrm{el,m}}$ is the electromechanical efficiency.

Energy balances for the valves, recondenser and mixer, and heat exchangers and economizer are depicted respectively in Eqs. (16), (17) and (18).

$$h_i = h_o \tag{16}$$

$$\sum_i \dot{m}_i h_i = \dot{m}_o h_o \tag{17}$$

$$\sum_i \dot{m}_i h_i = \sum_o \dot{m}_o h_o \tag{18}$$

The combustion process in the boiler is performed with 10 % excess air. Therefore, the balanced equation is:

$$\mathrm{CH_4} + \left(2 + \frac{1}{5}\right)\left(\mathrm{O_2} + \left(3 + \frac{16}{21}\right)\mathrm{N_2}\right) \rightarrow \frac{1}{5}\mathrm{O_2} + \mathrm{CO_2} + 2\mathrm{H_2O_{(g)}} + \left(8 + \frac{29}{105}\right)\mathrm{N_2} \tag{19}$$

The boiler heat flow rate ($\dot{Q}_{\mathrm{b}}$) is calculated as:

$$\dot{Q}_{\mathrm{b}} = \dot{Q}_{\mathrm{v}} + \dot{Q}_{\mathrm{ec}} \tag{20}$$

where $\dot{Q}_{\mathrm{v}}$ is the heat flow rate in the vaporizer section and $\dot{Q}_{\mathrm{ec}}$ that of the economizer.

Boiler efficiency (η_{b}) is defined as:

$$\eta_{\mathrm{b}} = \frac{\dot{Q}_{\mathrm{b}}}{\dot{m}_{\mathrm{BOG,b}} h_{\mathrm{LHV,BOG}}} \tag{21}$$

where $\dot{m}_{\mathrm{BOG,b}}$ is the BOG mass flow consumed by the boiler and $h_{\mathrm{LHV,BOG}}$ is the lower heating value of natural gas.

Eq. (22) establishes the energy balance of the combustion reaction that takes place in the boiler:

$$\left[(\eta_{\mathrm{comb}} - \eta_{\mathrm{b}})(h_{\mathrm{LHV,BOG}}) + \frac{\dot{Q}_{\mathrm{ec}}}{\dot{m}_{\mathrm{BOG,b}}}\right] M_{\mathrm{CH_4}} = \sum_{\mathrm{P}} n_o(\Delta\bar{h}_o) - \sum_{\mathrm{R}} n_i(\Delta\bar{h}_i) \tag{22}$$

where η_{comb} is the combustion efficiency, $M_{\mathrm{CH_4}}$ is the molar mass of methane and the other side of the equation represents the molar enthalpy change between the products and reactants.

The regasification system power ($\dot{W}_{\mathrm{RS}}$) and the FSRU electric output ($\dot{W}_{\mathrm{el,FSRU}}$) are defined in Eqs. (23) and (24) respectively. The base electric power ($\dot{W}_{\mathrm{el,b}}$) depicts the consumption of the ship's auxiliary services, including the fuel gas pump.

$$\dot{W}_{\mathrm{RS}} = \sum \dot{W}_{\mathrm{pumps}} + \sum \dot{W}_{\mathrm{comp}} \tag{23}$$

$$\dot{W}_{\mathrm{el,FSRU}} = \dot{W}_{\mathrm{el,b}} + \sum \dot{W}_{\mathrm{el,pumps}} + \sum \dot{W}_{\mathrm{el,comp}} \tag{24}$$

The power delivered by the engines ($\dot{W}_{\mathrm{eng}}$) can be calculated as:

$$\dot{W}_{\mathrm{eng}} = \frac{\dot{W}_{\mathrm{el,FSRU}}}{\eta_{\mathrm{alt}}} \tag{25}$$

where η_{alt} is the average efficiency of the alternators. Power is distributed between two engines: a 6L50DF and a 12V50DF. The load of each engine is assigned minimizing fuel consumption, as per Table 7.

Table 7
Engines load sharing as a function of the power delivered. Maximum engine power of 6L50DF ($\dot{W}_{\mathrm{6L,max}}$) and maximum engine power of 12V50DF ($\dot{W}_{\mathrm{12V,max}}$).

Conditions	**Load sharing**	
	6L50DF	**12V50DF**
$\dot{W}_{\mathrm{eng}} < 80\ \%\ \dot{W}_{\mathrm{6L,max}}$	$\dot{W}_{\mathrm{eng}}$	-
$80\ \%\ \dot{W}_{\mathrm{6L,max}} < \dot{W}_{\mathrm{eng}} < 80\ \%\ \dot{W}_{\mathrm{12V,max}}$	-	$\dot{W}_{\mathrm{eng}}$
$80\ \%\ \dot{W}_{\mathrm{6L,max}} < \dot{W}_{\mathrm{eng}}$ $\dot{W}_{\mathrm{eng}} < 12.5\ \%\ \dot{W}_{\mathrm{6L,max}} + 80\ \%\ \dot{W}_{\mathrm{12V,max}}$	$12.5\ \%\ \dot{W}_{\mathrm{6L,max}}$	$\dot{W}_{\mathrm{eng}} - \dot{W}_{\mathrm{6L}}$
$12.5\ \%\ \dot{W}_{\mathrm{6L,max}} + 80\ \%\ \dot{W}_{\mathrm{12V,max}} < \dot{W}_{\mathrm{eng}}$	$\dot{W}_{\mathrm{eng}} - \dot{W}_{\mathrm{12V}}$	$80\ \%\ \dot{W}_{\mathrm{12V,max}}$

The specific energy consumption of each fuel ($b_{\mathrm{f}(i)}$), considering the pilot diesel oil (DO) and natural gas, depends on the power developed by the engine ($\dot{W}_{\mathrm{eng}(i)}$):

$$b_{\mathrm{f}(i)} = f\left(\dot{W}_{\mathrm{eng}(i)}\right) \tag{26}$$

Hence the mass flow of fuel consumed ($\dot{m}_{\mathrm{f}(i)}$) is:

$$\dot{m}_{\mathrm{f}(i)} = \frac{b_{\mathrm{f}(i)}\dot{W}_{\mathrm{eng}(i)}}{h_{\mathrm{LHV,f}}} \tag{27}$$

where $h_{\mathrm{LHV,f}}$ is the lower heating value of the fuel. The total consumption of each fuel ($\dot{m}_{\mathrm{f,eng}}$) can be calculated using Eq. (28).

$$\dot{m}_{\mathrm{f,eng}} = \sum \dot{m}_{\mathrm{f}(i)} \tag{28}$$

The total energy flow rate supplied to the FSRU ($\dot{H}_{\mathrm{tot}}$) is defined as:

$$\dot{H}_{\mathrm{tot}} = (\dot{m}_{\mathrm{BOG,b}} + \dot{m}_{\mathrm{BOG,eng}})h_{\mathrm{LHV,BOG}} + \dot{m}_{\mathrm{DO,eng}}h_{\mathrm{LHV,DO}} \tag{29}$$

where $\dot{m}_{\mathrm{BOG,eng}}$ and $\dot{m}_{\mathrm{DO,eng}}$ are the BOG and DO mass flow rate consumed by the engine, and $h_{\mathrm{LHV,DO}}$ the DO lower heating value.

The efficiency of a regasification system (RS) can be measured in terms of specific power consumption (b_{RS}). Hence, power consumption per kilogram of regasified natural gas is calculated as:

$$b_{\mathrm{RS}} = \frac{\dot{W}_{\mathrm{RS}}}{\dot{m}_{\mathrm{NG}}} \tag{30}$$

Similarly, specific energy consumption in a FSRU (b_{FSRU}) can be defined as:

$$b_{\mathrm{FSRU}} = \frac{\dot{H}_{\mathrm{tot}}}{\dot{m}_{\mathrm{NG}}} \tag{31}$$

3.4 Exergy analysis

The exergy analysis determines exergy (useful work) destruction caused by irreversibilities in the different components of a system. It is, therefore, a more convenient and appropriate method than energy analysis when evaluating efficiency and identifying which components can be improved.

Exergy can be divided into four terms: physical, chemical, potential, and kinetic exergy. Disregarding the potential and kinetic terms, the specific flow exergy (e) is defined by:

$$e = e^{\mathrm{ph}} + e^{\mathrm{ch}} \tag{32}$$

where e^{ph} is the physical component and e^{ch} the chemical one.

The physical exergy, also termed thermomechanical, is calculated with Eq. (21). In this case, subscript 0 refers to the pressure and temperature conditions of the reference state.

$$e^{\mathrm{ph}} = h - h_0 - T_0(s - s_0) \tag{33}$$

Furthermore, physical exergy can be decomposed into thermal (e^{th}) and mechanical (e^{p}): exergy:

$$e^{\mathrm{ph}} = e^{\mathrm{th}} + e^{\mathrm{p}} \tag{34}$$

However, the unequivocal determination of physical components is only possible for ideal gases and incompressible fluids [35]. For any fluid, thermal and mechanical exergy are usually defined as:

$$e^{\mathrm{th}} = e^{\mathrm{ph}}(T, p) - e^{\mathrm{ph}}(T_0, p) \tag{35}$$

$$e^{\mathrm{p}} = e^{\mathrm{ph}}(T_0, p) - e^{\mathrm{ph}}(T_0, p_0) \tag{36}$$

The standard chemical exergies of the fluids used in this study are listed in Table 8 [28]. The chemical exergy of the BOG ($e^{\mathrm{ch}}_{\mathrm{BOG}}$), DO ($e^{\mathrm{ch}}_{\mathrm{DO}}$) and of gas mixtures present in the atmosphere ($e^{\mathrm{ch}}_{\mathrm{m}}$), that is, air and gas phase of flue gases, are calculated with Eqs. (37), (38) and (39) respectively. The values used for the factors φ_{BOG} and φ_{DO} are 1.04 and 1.07 [28].

$$e^{\mathrm{ch}}_{\mathrm{BOG}} = \varphi_{\mathrm{BOG}} h_{\mathrm{LHV,BOG}} \tag{37}$$

$$e^{\mathrm{ch}}_{\mathrm{DO}} = \varphi_{\mathrm{DO}} h_{\mathrm{LHV,DO}} \tag{38}$$

$$e^{\mathrm{ch}}_{\mathrm{m}} = \frac{1}{M_{\mathrm{m}}}\left[\sum_i y_i \bar{e}^{\mathrm{ch}}_i + \bar{R} T_0 \sum_i y_i \ln(y_i)\right] \tag{39}$$

where M_{m} is the molar mass of the gas mixture, y_i is the mole fraction of each component i in the mixture and $\bar{R}$ the universal gas constant.

The flue gases of the boiler at the reference state are composed of gases, water vapour and liquid water. For this case, the chemical exergy of the mixture ($e_{\mathrm{m}}^{\mathrm{ch}}$) is determined as follows [36]:

$$e_{\mathrm{m}}^{\mathrm{ch}} = \frac{1}{M_{\mathrm{m}}}\left(y_{\mathrm{g}}\bar{e}_{\mathrm{g}}^{\mathrm{ch}} + y_{\mathrm{l}}\bar{e}_{\mathrm{l}}^{\mathrm{ch}}\right) \tag{40}$$

where y_{g} is the mole fraction of the gas phase, $\bar{e}_{\mathrm{g}}^{\mathrm{ch}}$ is the molar chemical exergy of the gas phase calculated with Eq. (39), y_{l} is the mole fraction of the liquid water and $\bar{e}_{\mathrm{l}}^{\mathrm{ch}}$ is the molar chemical exergy of the liquid water.

The exergy destroyed by pumps and compressors, valves, the recondenser and mixer, heat exchangers and the economizer, as well as the boiler, are determined respectively with Eqs. (41), (42), (43), (44) and (45).

$$\dot{I} = \dot{W} - \dot{m}(e_o - e_i) \tag{41}$$

$$\dot{I} = \dot{m}(e_i - e_o) \tag{42}$$

$$\dot{I} = \sum_i \dot{m}_i e_i - \dot{m}_o e_o \tag{43}$$

$$\dot{I} = \sum_i \dot{m}_i e_i - \sum_o \dot{m}_o e_o \tag{44}$$

$$\dot{I} = \left[\left(\dot{m}_{\mathrm{air}} e_{\mathrm{air}} + \dot{m}_{\mathrm{BOG,b}} e_{\mathrm{BOG,b}}\right) - \dot{m}_P e_P\right] - \left[\dot{m}_{\mathrm{water}}(e_o - e_i)\right] \tag{45}$$

The exergy efficiency of pumps and compressors is:

$$\eta_{\mathrm{ex}} = \frac{\dot{m}(e_o - e_i)}{\dot{W}} \tag{46}$$

The exergy efficiency of heat exchangers is determined as follows:

$$\eta_{\mathrm{ex}} = \frac{[\dot{m}(e_o - e_i)]_{\mathrm{product}}}{[\dot{m}(e_i - e_o)]_{\mathrm{supply}}} \tag{47}$$

Eq. (47) is applicable to the mixer (pre-cooling) and recondenser as they operate as open heat exchangers.

The exergy efficiency of the boiler can be defined as:

$$\eta_{\mathrm{ex}} = \frac{\dot{m}_{\mathrm{water}}(e_o - e_i)}{\left(\dot{m}_{\mathrm{air}} e_{\mathrm{air}} + \dot{m}_{\mathrm{BOG,b}} e_{\mathrm{BOG,b}}\right) - \dot{m}_P e_P} \tag{48}$$

Valves and steam traps, being dissipative components, are combined with the nearest heat exchangers to determine the exergy efficiency of the subsystem.

Table 8
Standard chemical exergy of fluids [28].

Substance	Standard chemical exergy	
	(kJ/kmol)	(kJ/kg)
Nitrogen	720.00	25.70
Oxygen	3970.00	124.07
Water (gas)	9500.00	527.31
Water (liquid)	900.00	49.96
Carbon dioxide	19 870.00	451.49
NG	825 893.64	51 480.00
DO	-	45 689.00
Air $(21\ \%\ O_2 + 79\ \%\ N_2)_{mole}$	128.44	4.45
Flue gases (boiler) $(1.74\ \%\ O_2 + 8.71\ \%\ CO_2 + 2.67\ \%\ H_2O_{(g)} + 14.76\ \%\ H_2O_{(l)} + 72.12\ \%\ N_2)_{mole}$	1517.44	54.72

3.4.1 Exergy efficiency of the regasification systems

Figure 4 illustrates the exergies involved in the balance of a regasification system.

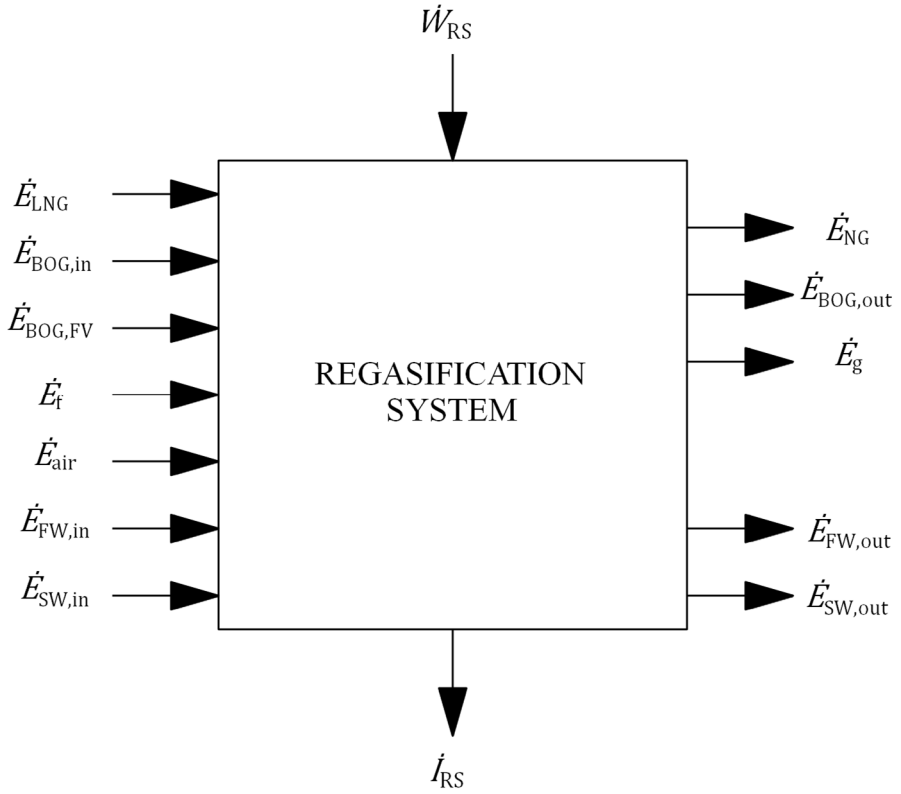

Figure 4. Exergy balance of a regasification system.

The FV and fuel gas pump are excluded from the balance. Therefore, there are no irreversibilities associated with said components. The exergy balance of a regasification system can be defined as:

$$\dot{I}_{RS} = \left(\dot{E}_{LNG} + \dot{E}_{BOG,in} + \dot{E}_{BOG,FV} + \dot{E}_{f} + \dot{E}_{air} + \dot{E}_{FW,in} + \dot{E}_{SW,in}\right) + \dot{W}_{RS} - \left(\dot{E}_{NG} + \dot{E}_{BOG,out} + \dot{E}_{g} + \dot{E}_{FW,out} + \dot{E}_{SW,out}\right) \quad (49)$$

where $\dot{I}_{RS}$ is the exergy destroyed due to irreversibilities in the regasification system; $\dot{E}_{LNG}$ is the exergy of the LNG entering the system (including the exergy of the LNG flow from the mixer); $\dot{E}_{BOG,in}$ is the exergy of the BOG from the tanks; $\dot{E}_{BOG,FV}$ is the exergy of the BOG leaving the FV; $\dot{E}_{f}$ is the exergy of fuels, other than BOG, used in combustion for the regasification process; $\dot{E}_{air}$ is the exergy of air at ambient temperature and pressure for combustion processes; $\dot{E}_{FW,in}$ is the exergy of the fresh cooling water entering the AC/NGH; $\dot{E}_{SW,in}$ is the exergy of the seawater entering the regasification system; $\dot{W}_{RS}$ is the power supplied to the regasification system; $\dot{E}_{NG}$ is the regasified natural gas exergy; $\dot{E}_{BOG,out}$ is the exergy of the BOG exiting the regasification system (BOG used by other

equipment, for example, DFDE engines); $\dot{E}_{\mathrm{g}}$ is the exergy of the gases produced by the combustion processes; $\dot{E}_{\mathrm{FW,out}}$ is the exergy of the fresh cooling water exiting the AC/NGH, and $\dot{E}_{\mathrm{SW,out}}$is the exergy of the seawater leaving the regasification system.

The process that takes place in a regasification system is characterized by being an exergy destroyer. In other words, despite supplying power to the system, the exergy variation between the flows that leave and those that enter is negative in value. This implies that the exergy efficiency of the system cannot be obtained with the terms used in Eq. (49), but rather a further analysis of the exergetic terms of natural gas is required. The breakdown of exergies related to the natural gas fluid of Eq. (49) in thermal, mechanical and chemical exergy yields:

$$\begin{aligned}\dot{I}_{\mathrm{RS}} = &\left[\left(\dot{E}^{\mathrm{p}}_{\mathrm{LNG}} + \dot{E}^{\mathrm{p}}_{\mathrm{BOG,in}} + \dot{E}^{\mathrm{p}}_{\mathrm{BOG,FV}}\right) - \left(\dot{E}^{\mathrm{p}}_{\mathrm{NG}} + \dot{E}^{\mathrm{p}}_{\mathrm{BOG,out}}\right)\right] \\ &+\left[\left(\dot{E}^{\mathrm{th}}_{\mathrm{LNG}} + \dot{E}^{\mathrm{th}}_{\mathrm{BOG,in}} + \dot{E}^{\mathrm{th}}_{\mathrm{BOG,FV}}\right) - \left(\dot{E}^{\mathrm{th}}_{\mathrm{NG}} + \dot{E}^{\mathrm{th}}_{\mathrm{BOG,out}}\right)\right] \\ &+\left[\left(\dot{E}^{\mathrm{ch}}_{\mathrm{LNG}} + \dot{E}^{\mathrm{ch}}_{\mathrm{BOG,in}} + \dot{E}^{\mathrm{ch}}_{\mathrm{BOG,FV}}\right) - \left(\dot{E}^{\mathrm{ch}}_{\mathrm{NG}} + \dot{E}^{\mathrm{ch}}_{\mathrm{BOG,out}}\right)\right] \\ &+\dot{E}_{\mathrm{f}} + \dot{E}_{\mathrm{air}} - \dot{E}_{\mathrm{g}} \\ &+\left(\dot{E}_{\mathrm{FW,in}} - \dot{E}_{\mathrm{FW,out}}\right) \\ &+\left(\dot{E}_{\mathrm{SW,in}} - \dot{E}_{\mathrm{SW,out}}\right) \\ &+\dot{W}_{\mathrm{RS}}\end{aligned} \tag{50}$$

Some terms in the above equation can be replaced considering the following relationships:

$$\Delta\dot{E}^{\mathrm{p}}_{\mathrm{NG}} = -\left[\left(\dot{E}^{\mathrm{p}}_{\mathrm{LNG}} + \dot{E}^{\mathrm{p}}_{\mathrm{BOG,in}} + \dot{E}^{\mathrm{p}}_{\mathrm{BOG,FV}}\right) - \left(\dot{E}^{\mathrm{p}}_{\mathrm{NG}} + \dot{E}^{\mathrm{p}}_{\mathrm{BOG,out}}\right)\right] \tag{51}$$

$$\Delta\dot{E}^{\mathrm{th}}_{\mathrm{NG}} = -\left[\left(\dot{E}^{\mathrm{th}}_{\mathrm{LNG}} + \dot{E}^{\mathrm{th}}_{\mathrm{BOG,in}} + \dot{E}^{\mathrm{th}}_{\mathrm{BOG,FV}}\right) - \left(\dot{E}^{\mathrm{th}}_{\mathrm{NG}} + \dot{E}^{\mathrm{th}}_{\mathrm{BOG,out}}\right)\right] \tag{52}$$

$$\Delta\dot{E}^{\mathrm{ch}}_{\mathrm{NG}} = -\left[\left(\dot{E}^{\mathrm{ch}}_{\mathrm{LNG}} + \dot{E}^{\mathrm{ch}}_{\mathrm{BOG,in}} + \dot{E}^{\mathrm{ch}}_{\mathrm{BOG,FV}}\right) - \left(\dot{E}^{\mathrm{ch}}_{\mathrm{NG}} + \dot{E}^{\mathrm{ch}}_{\mathrm{BOG,out}}\right)\right] \tag{53}$$

$$\Delta\dot{E}_{\mathrm{FW}} = -\left(\dot{E}_{\mathrm{FW,in}} - \dot{E}_{\mathrm{FW,out}}\right) \tag{54}$$

$$\Delta\dot{E}_{\mathrm{SW}} = -\left(\dot{E}_{\mathrm{SW,in}} - \dot{E}_{\mathrm{SW,out}}\right) \tag{55}$$

Introducing the previous terms in Eq. (50) gives:

$$\dot{I}_{\mathrm{RS}} + \Delta\dot{E}^{\mathrm{p}}_{\mathrm{NG}} + \Delta\dot{E}_{\mathrm{SW}} = \left(\dot{E}_{\mathrm{f}} + \dot{E}_{\mathrm{air}} - \Delta\dot{E}^{\mathrm{ch}}_{\mathrm{NG}} - \dot{E}_{\mathrm{g}}\right) - \left(\Delta\dot{E}^{\mathrm{th}}_{\mathrm{NG}} + \Delta\dot{E}_{\mathrm{FW}}\right) + \dot{W}_{\mathrm{RS}} \tag{56}$$

In Eq. (56) all exergy variations are negative in value, except for those variations associated with natural gas mechanical exergy and seawater exergy. That is, the regasification system is supplied with exergy from the combustion process (terms in the first parentheses), LNG thermal exergy, exergy from cooling water and power consumed by pumps and compressors. In return, natural gas mechanical exergy and seawater thermal exergy are increased but at a cost of several irreversibilities.

Considering Eq. (56), the exergy efficiency of a regasification system ($\eta_{\mathrm{ex,RS}}$) can be defined as:

$$\eta_{\mathrm{ex,RS}} = \frac{\Delta\dot{E}_{\mathrm{NG}}^{\mathrm{p}} + \Delta\dot{E}_{\mathrm{SW}}}{\left(\dot{E}_{\mathrm{f}} + \dot{E}_{\mathrm{air}} - \Delta\dot{E}_{\mathrm{NG}}^{\mathrm{ch}} - \dot{E}_{\mathrm{g}}\right) - \left(\Delta\dot{E}_{\mathrm{NG}}^{\mathrm{th}} + \Delta\dot{E}_{\mathrm{FW}}\right) + \dot{W}_{\mathrm{RS}}} \tag{57}$$

3.4.2 Exergy efficiency of FSRUs (regasifying)

FRSU exergy efficiency can be determined considering the definition developed for regasification systems. Figure 5 illustrates the exergies involved in the balance for FSRU regasifying.

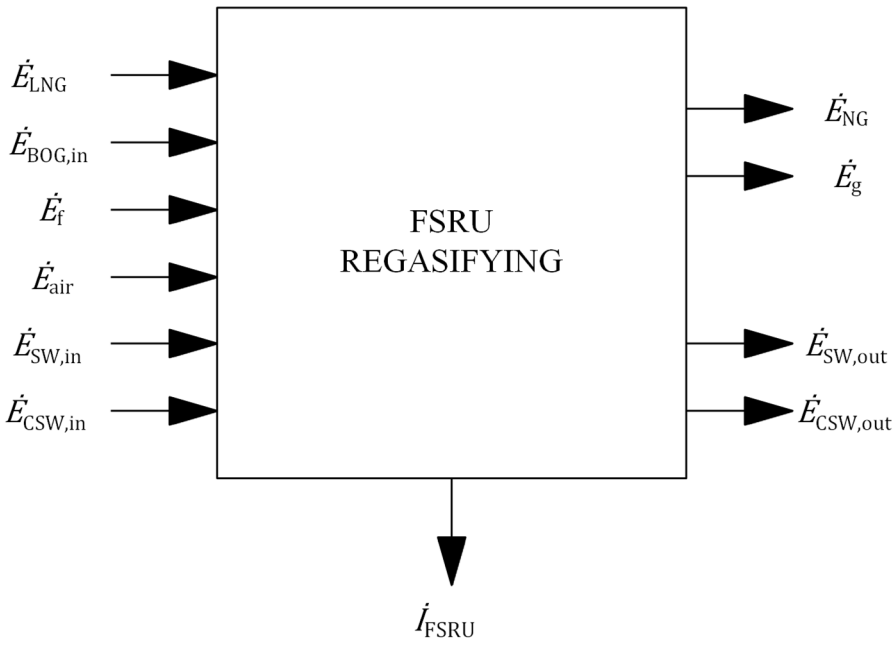

Figure 5. Exergy balance of a FSRU.

The FSRU exergy balance is as follows:

$$\dot{I}_{\mathrm{FSRU}} = \left(\dot{E}_{\mathrm{LNG}} + \dot{E}_{\mathrm{BOG,in}} + \dot{E}_{\mathrm{f}} + \dot{E}_{\mathrm{air}} + \dot{E}_{\mathrm{SW,in}} + \dot{E}_{\mathrm{CSW,in}}\right) - \left(\dot{E}_{\mathrm{NG}} + \dot{E}_{\mathrm{g}} + \dot{E}_{\mathrm{SW,out}} + \dot{E}_{\mathrm{CSW,out}}\right) \tag{58}$$

where $\dot{I}_{\mathrm{FSRU}}$ is the exergy destroyed owing to irreversibilities in the FSRU; $\dot{E}_{\mathrm{LNG}}$ is the exergy of the LNG flow leaving the tanks; $\dot{E}_{\mathrm{BOG,in}}$ is the exergy of the BOG received from the tanks; $\dot{E}_{\mathrm{f}}$ is the fuel exergy, with the exclusion of BOG, used in combustion processes; $\dot{E}_{\mathrm{air}}$ is the air exergy for combustion processes; $\dot{E}_{\mathrm{SW,in}}$ is the exergy of the seawater at the regasification system inlet; $\dot{E}_{\mathrm{CSW,in}}$ is the exergy of seawater entering the vessel's cooling system; $\dot{E}_{\mathrm{NG}}$ is the regasified natural gas exergy; $\dot{E}_{\mathrm{g}}$ is the exergy of the gases produced by the combustion processes; $\dot{E}_{\mathrm{SW,out}}$ is the exergy of the seawater exiting the regasification system, and $\dot{E}_{\mathrm{CSW,out}}$ is the exergy of the seawater discharged by the vessel's cooling system.

The following is obtained upon decomposing the exergies associated with natural gas:

$$\begin{aligned}\dot{I}_{\mathrm{FSRU}} = &\left[\left(\dot{E}^{\mathrm{p}}_{\mathrm{LNG}} + \dot{E}^{\mathrm{p}}_{\mathrm{BOG,in}}\right) - \left(\dot{E}^{\mathrm{p}}_{\mathrm{NG}}\right)\right] \\ &+\left[\left(\dot{E}^{\mathrm{th}}_{\mathrm{LNG}} + \dot{E}^{\mathrm{th}}_{\mathrm{BOG,in}}\right) - \left(\dot{E}^{\mathrm{th}}_{\mathrm{NG}}\right)\right] \\ &+\left[\left(\dot{E}^{\mathrm{ch}}_{\mathrm{LNG}} + \dot{E}^{\mathrm{ch}}_{\mathrm{BOG,in}}\right) - \left(\dot{E}^{\mathrm{ch}}_{\mathrm{NG}}\right)\right] \\ &+\dot{E}_{\mathrm{f}} + \dot{E}_{\mathrm{air}} - \dot{E}_{\mathrm{g}} \\ &+\left(\dot{E}_{\mathrm{SW,in}} - \dot{E}_{\mathrm{SW,out}}\right) \\ &+\left(\dot{E}_{\mathrm{CSW,in}} - \dot{E}_{\mathrm{CSW,out}}\right)\end{aligned} \tag{59}$$

Some terms can be replaced considering the following relationships:

$$\Delta\dot{E}^{\mathrm{p}}_{\mathrm{NG}} = -\left[\left(\dot{E}^{\mathrm{p}}_{\mathrm{LNG}} + \dot{E}^{\mathrm{p}}_{\mathrm{BOG,in}}\right) - \left(\dot{E}^{\mathrm{p}}_{\mathrm{NG}}\right)\right] \tag{60}$$

$$\Delta\dot{E}^{\mathrm{th}}_{\mathrm{NG}} = -\left[\left(\dot{E}^{\mathrm{th}}_{\mathrm{LNG}} + \dot{E}^{\mathrm{th}}_{\mathrm{BOG,in}}\right) - \left(\dot{E}^{\mathrm{th}}_{\mathrm{NG}}\right)\right] \tag{61}$$

$$\Delta\dot{E}^{\mathrm{ch}}_{\mathrm{NG}} = -\left[\left(\dot{E}^{\mathrm{ch}}_{\mathrm{LNG}} + \dot{E}^{\mathrm{ch}}_{\mathrm{BOG,in}}\right) - \left(\dot{E}^{\mathrm{ch}}_{\mathrm{NG}}\right)\right] \tag{62}$$

$$\Delta\dot{E}_{\mathrm{SW}} = -\left(\dot{E}_{\mathrm{SW,in}} - \dot{E}_{\mathrm{SW,out}}\right) \tag{63}$$

$$\Delta\dot{E}_{\mathrm{CSW}} = -\left(\dot{E}_{\mathrm{CSW,in}} - \dot{E}_{\mathrm{CSW,out}}\right) \tag{64}$$

Substituting in Eq. (59) yields:

$$\dot{I}_{\mathrm{FSRU}} + \Delta\dot{E}^{\mathrm{p}}_{\mathrm{NG}} + \Delta\dot{E}_{\mathrm{CSW}} + \Delta\dot{E}_{\mathrm{SW}} = \left(\dot{E}_{\mathrm{f}} + \dot{E}_{\mathrm{air}} - \Delta\dot{E}^{\mathrm{ch}}_{\mathrm{NG}} - \dot{E}_{\mathrm{g}}\right) - \left(\Delta\dot{E}^{\mathrm{th}}_{\mathrm{NG}}\right) \tag{65}$$

If the following conditions are assumed:

- Composition of the air used in the engine combustion process is identical to that of the reference state.
- The gases, emerging from the combustion processes, reach ambient reference state.
- Seawater discharged by the ship's systems returns to the conditions in which it was supplied.

The consequences of the above conditions are as follows:

- The chemical exergy of air ($\dot{E}^{\mathrm{ch}}_{\mathrm{air}}$) is non-zero for those combustion processes unconnected to the engines and whose composition is different to that of the reference state.
- The exergy of the gases $\dot{E}_{\mathrm{g}}$ and the exergy variations $\Delta\dot{E}_{\mathrm{SW}}$ and $\Delta\dot{E}_{\mathrm{CSW}}$ are equal to zero.

Consequently, the exergy efficiency of a FSRU ($\eta_{\mathrm{ex,FSRU}}$) is:

$$\eta_{\mathrm{ex,FSRU}} = \frac{\Delta\dot{E}^{\mathrm{p}}_{\mathrm{NG}}}{\left(\dot{E}_{\mathrm{f}} + \dot{E}_{\mathrm{air}} - \Delta\dot{E}^{\mathrm{ch}}_{\mathrm{NG}}\right) - \Delta\dot{E}^{\mathrm{th}}_{\mathrm{NG}}} \tag{66}$$

3.5 Economic analysis

The economic assessment focuses on the study of regasification modules since most of the remaining components that comprise the FSRU are common. In this case, a module contains two booster pumps and the exchangers or intermediate circuit components that intervene in the LNG regasification process. The associated financial investment for the components of each regasification system is calculated for three identical regasification modules, each with a maximum capacity of 250 mmscfd. The simulation of the regasification process, the sizing of the exchangers and the evaluation of the costs of each system were performed respectively with the Aspen HYSYS, Aspen EDR and APEA, programs that are part of the AspenONE suite. The Peng-Robinson equation of state was applied to determine the properties of the fluids in the above programs. The method developed in the economic evaluation of regasification systems is described below.

The cost rate of any regasification system installed in a FSRU ($\dot{C}_{\mathrm{tot}}$) can be defined as:

$$\dot{C}_{\mathrm{tot}} = \dot{C}_{\mathrm{f,tot}} + \dot{Z}_{\mathrm{tot}}^{\mathrm{CI}} + \dot{Z}_{\mathrm{tot}}^{\mathrm{OM}} \tag{67}$$

where $\dot{C}_{\mathrm{f,tot}}$ is the cost rate associated with fuels, $\dot{Z}_{\mathrm{tot}}^{\mathrm{CI}}$ is the capital investment cost rate and $\dot{Z}_{\mathrm{tot}}^{\mathrm{OM}}$ is the operation and maintenance cost rate.

The sum of rates $\dot{Z}_{\mathrm{tot}}^{\mathrm{CI}}$ and $\dot{Z}_{\mathrm{tot}}^{\mathrm{OM}}$ is determined with the following equation [36]:

$$\dot{Z}_{\mathrm{tot}}^{\mathrm{CI}} + \dot{Z}_{\mathrm{tot}}^{\mathrm{OM}} = \frac{Z_{\mathrm{tot}}^{\mathrm{CI}}(\gamma_{\mathrm{OM}} + \beta_{\mathrm{CRF}})}{\tau} \tag{68}$$

where $Z_{\mathrm{tot}}^{\mathrm{CI}}$ is the capital investment cost of the regasification system, γ_{OM} is the operation and maintenance factor, β_{CRF} is the capital recovery factor calculated in Eq. (69) based on the annual interest (i) and the estimated lifetime of the regasification system (n), and τ is the annual operating hours.

$$\beta_{\mathrm{CRF}} = \frac{i(1+i)^n}{(1+i)^n - 1} \tag{69}$$

The cost of capital investment of the regasification system is updated to 2019 by means of the CEPCI with the following equation:

$$Z_{\mathrm{tot}}^{\mathrm{CI}} = \frac{CEPCI_{2019}}{CEPCI_{\mathrm{March,2018}}} (FCI)_{\mathrm{March,2018}} \tag{70}$$

where FCI is the fixed capital investment, also known as the total project or capital cost, calculated with the APEA program and whose reference date is March 2018 [37].

Table 9 lists the parameters required for the economic assessment.

Table 9
Economic analysis parameters.

Parameter	**Value**
γ_{OM}	3 % [38]
i	12 % [36]
n	20 years [22]
τ	8000 hours
$CEPCI_{\mathrm{March,2018}}$	588 [39]
$CEPCI_{2019}$	607.5 [39]
DO price	500 USD/t [40]
LNG price	1-11 USD/MMBtu

4 Results and discussion

The thermodynamics (energy and exergy) and economics results obtained from the study of the regasification systems are discussed below in sections 4.1 and 4.2, respectively.

4.1 Thermodynamics

The main thermodynamic properties of the analysed regasification systems are depicted in Table 10, Table 11 and Table 12. In addition, Table 13, Table 14 and Table 15 provide the composition of the selected states. Figure 6-Figure 8 illustrate the regasification process of each system in an e^{ph}-h diagram. This type of diagram allows us to easily observe of the development of physical exergy and of the thermal and mechanical components without disregarding enthalpy. That is, the processes can be analysed simultaneously in terms of both energy and exergy. Unlike the open loop regasification systems studied, BOG consumption is far greater in the closed loop water-glycol system for the same regasified natural gas flow. The high consumption of BOG causes the absence of BOG excess. That is, the natural BOG generated by the transfer of heat from the environment to the tanks is not enough to maintain the pressure therein. Consequently, the recondenser must operate as a suction tank (see Figure 8a) and, additionally, LNG requires vaporization in the FV. While on the other hand LNG temperature at the recondenser outlet in all three regasification systems analysed is low enough to avoid cavitation problems in the booster pump. At worst, which corresponds to the seawater regasification system (Figure 6), LNG temperature at the recondenser outlet reaches -158.77 ºC, meaning a temperature difference of 22.67 ºC concerning to the point of saturated liquid at the same pressure.

Table 10
Thermodynamic data of the seawater regasification system.

State	Fluid	T (°C)	p (bar)	h (kJ/kg)	s (kJ/kg-K)	e^{ph} (kJ/kg)	$\dot{m}$ (kg/s)
1	LNG	-159.78	1.16325	-904.96	-6.624	1070.27	110.96
2	LNG	-159.43	9.00	-902.63	-6.620	1071.37	110.96
3	LNG	-159.29	5.50	-902.63	-6.613	1069.19	110.96
4	LNG	-158.77	5.50	-900.81	-6.597	1066.27	111.19
5	LNG	-154.18	110.00	-869.84	-6.544	1081.60	111.19
6	NG	10.00	85.00	-130.38	-2.664	664.10	111.19
7	LNG	-159.78	1.16325	-904.96	-6.624	1070.27	0.05
8	LNG	-159.78	1.16325	-904.96	-6.624	1070.27	0.05
9	BOG	-120.00	1.16325	-311.42	-1.496	134.92	0.00
10	BOG	-100.00	1.16325	-269.13	-1.237	99.82	0.69
11	BOG	-120.00	1.16325	-311.42	-1.496	134.92	0.74
12	BOG	16.84	6.00	-24.26	-0.999	273.75	0.74
13	BOG	16.61	5.50	-24.26	-0.954	260.45	0.23
14	BOG	35.35	5.90	17.73	-0.850	271.32	0.51
15	SW	15.00	1.01325	59.94	0.214	0.77	3981.81
16	SW	15.05	7.50	60.73	0.214	1.40	3981.81
17	SW	10.00	1.01325	40.08	0.144	1.71	3981.81
18	FW	36.00	2.50	151.03	0.519	0.98	8.33
19	FW	35.39	2.35	148.48	0.510	0.87	8.33

Table 11
Thermodynamic data of the open loop propane regasification system.

State	Fluid	T (ºC)	p (bar)	h (kJ/kg)	s (kJ/kg-K)	e^{ph} (kJ/kg)	$\dot{m}$ (kg/s)
1	LNG	-159.78	1.16325	-904.96	-6.624	1070.27	110.97
2	LNG	-159.43	9.00	-902.63	-6.620	1071.37	110.97
3	LNG	-159.29	5.50	-902.63	-6.613	1069.19	110.97
4	LNG	-158.78	5.50	-900.86	-6.597	1066.34	111.19
5	LNG	-154.20	110.00	-869.89	-6.545	1081.67	111.19
6	NG	-20.00	87.00	-231.58	-3.052	678.60	111.19
7	NG	10.00	85.00	-130.38	-2.664	664.10	111.19
8	LNG	-159.78	1.16325	-904.96	-6.624	1070.27	0.05
9	LNG	-159.78	1.16325	-904.96	-6.624	1070.27	0.05
10	BOG	-120.00	1.16325	-311.42	-1.496	134.92	0.00
11	BOG	-100.00	1.16325	-269.13	-1.237	99.82	0.69
12	BOG	-120.00	1.16325	-311.42	-1.496	134.92	0.74
13	BOG	16.84	6.00	-24.26	-0.999	273.75	0.74
14	BOG	16.61	5.50	-24.26	-0.954	260.45	0.22
15	BOG	35.34	5.90	17.70	-0.850	271.32	0.51
16	Propane	-15.00	3.50	163.11	0.862	123.89	206.67
17	Propane	-14.84	6.00	163.68	0.862	124.33	206.67
18	Propane	4.92	5.50	506.54	2.102	97.53	206.67
19	SW	15.00	1.01325	59.94	0.214	0.77	3976.38
20	SW	15.05	7.50	60.73	0.214	1.40	3976.38
21	SW	10.00	1.01325	40.08	0.144	1.71	544.91
22	SW	10.00	1.01325	40.08	0.144	1.71	3431.47
23	FW	36.00	2.50	151.03	0.519	0.98	8.33
24	FW	35.38	2.35	148.45	0.510	0.87	8.33

Table 12
Thermodynamic data of the closed loop water-glycol regasification system.

State	Fluid	T (ºC)	p (bar)	h (kJ/kg)	s (kJ/kg-K)	e^{ph} (kJ/kg)	$\dot{m}$ (kg/s)
1	LNG	-159.78	1.16325	-904.96	-6.624	1070.27	111.19
2	LNG	-159.43	9.00	-902.63	-6.620	1071.37	111.19
3	LNG	-159.29	5.50	-902.63	-6.613	1069.19	111.19
4	LNG	-159.29	5.50	-902.63	-6.613	1069.19	111.19
5	LNG	-154.73	110.00	-871.70	-6.560	1084.42	111.19
6	NG	10.00	85.00	-130.38	-2.664	664.10	111.19
7	LNG	-159.78	1.16325	-904.96	-6.624	1070.27	1.60
8	LNG	-159.78	1.16325	-904.96	-6.624	1070.27	0.05
9	BOG	-120.00	1.16325	-311.42	-1.496	134.92	1.55
10	BOG	-100.00	1.16325	-269.13	-1.237	99.82	0.68
11	BOG	-120.00	1.16325	-311.42	-1.496	134.92	2.27
12	BOG	16.84	6.00	-24.26	-0.999	273.75	2.27
13	BOG	16.61	5.50	-24.26	-0.954	260.45	0.00
14	BOG	31.82	5.90	9.70	-0.876	271.10	2.27
15	BOG	31.82	5.90	9.70	-0.876	271.10	0.37
16	BOG	29.80	1.06	9.70	0.008	7.51	1.90
17	WG	25.00	3.50	61.18	0.000	0.24	331.66
18	WG	25.02	6.00	61.49	0.000	0.48	331.66
19	WG	90.00	5.50	309.72	0.753	24.30	331.66
20	Water	90.00	1.01325	377.06	1.193	25.98	37.98
21	Water	90.35	29.00	380.69	1.195	29.01	37.98
22	Water	135.00	29.00	569.46	1.685	71.76	37.98
23	Water	226.98	29.00	976.09	2.582	210.91	37.98
24	Water	231.98	29.00	2803.08	6.199	959.46	37.98
25	Water	225.28	25.50	2803.08	6.250	944.17	30.75
26	Water	30.02	2.50	126.03	0.437	0.32	30.75

Table 12
Thermodynamic data of the closed loop water-glycol regasification system.

State	Fluid	T (ºC)	p (bar)	h (kJ/kg)	s (kJ/kg-K)	e^{ph} (kJ/kg)	$\dot{m}$ (kg/s)
27	Water	30.05	1.01325	126.03	0.437	0.18	30.75
28	Water	187.13	9.00	2803.08	6.687	813.78	3.48
29	Water	175.35	9.00	742.56	2.094	122.78	3.48
30	Water	99.97	1.01325	742.56	2.174	98.96	3.48
31	Water	187.13	9.00	2803.08	6.687	813.78	3.75
32	Water	175.35	9.00	742.56	2.094	122.78	3.75
33	Water	99.97	1.01325	742.56	2.174	98.96	3.75
34	Water	90.00	1.01325	377.06	1.193	25.98	7.23
35	Air	25.00	1.01325	0.00	6.884	0.00	35.87
36	Air	30.16	1.06325	5.21	6.888	4.19	35.87
37	Gases	528.93	1.01325	-2166.81	8.357	262.60	37.78
38	Gases	185.88	1.01325	-2575.61	7.695	51.34	37.78
39	FW	36.00	2.50	151.03	0.519	0.98	8.33
40	FW	33.79	2.35	141.76	0.489	0.66	8.33
41	FW	36.00	2.50	151.03	0.519	0.98	79.03
42	FW	44.00	2.35	184.45	0.625	2.56	79.03

Table 13
Composition of the seawater regasification system states.

State	Composition (mole fraction %)							
	CH_4	C_3H_8	Sea water	CO_2	H_2O	O_2	N_2	EG
1	100	0	0	0	0	0	0	0
10	100	0	0	0	0	0	0	0
15	0	0	100	0	0	0	0	0
18	0	0	0	0	100	0	0	0

Table 14
Composition of the open loop propane regasification system states.

State	Composition (mole fraction %)							
	CH_4	**C_3H_8**	**Sea water**	**CO_2**	**H_2O**	**O_2**	**N_2**	**EG**
1	100	0	0	0	0	0	0	0
11	100	0	0	0	0	0	0	0
16	0	100	0	0	0	0	0	0
19	0	0	100	0	0	0	0	0
23	0	0	0	0	100	0	0	0

Table 15
Composition of the closed loop water-glycol regasification system states.

State	Composition (mole fraction %)							
	CH_4	**C_3H_8**	**Sea water**	**CO_2**	**H_2O**	**O_2**	**N_2**	**EG**
1	100	0	0	0	0	0	0	0
10	100	0	0	0	0	0	0	0
17	0	0	0	0	88.94	0	0	11.06
20	0	0	0	0	100	0	0	0
35	0	0	0	0	0	21.00	79.00	0
37	0	0	0	8.71	17.43	1.74	72.12	0
39	0	0	0	0	100	0	0	0
41	0	0	0	0	100	0	0	0

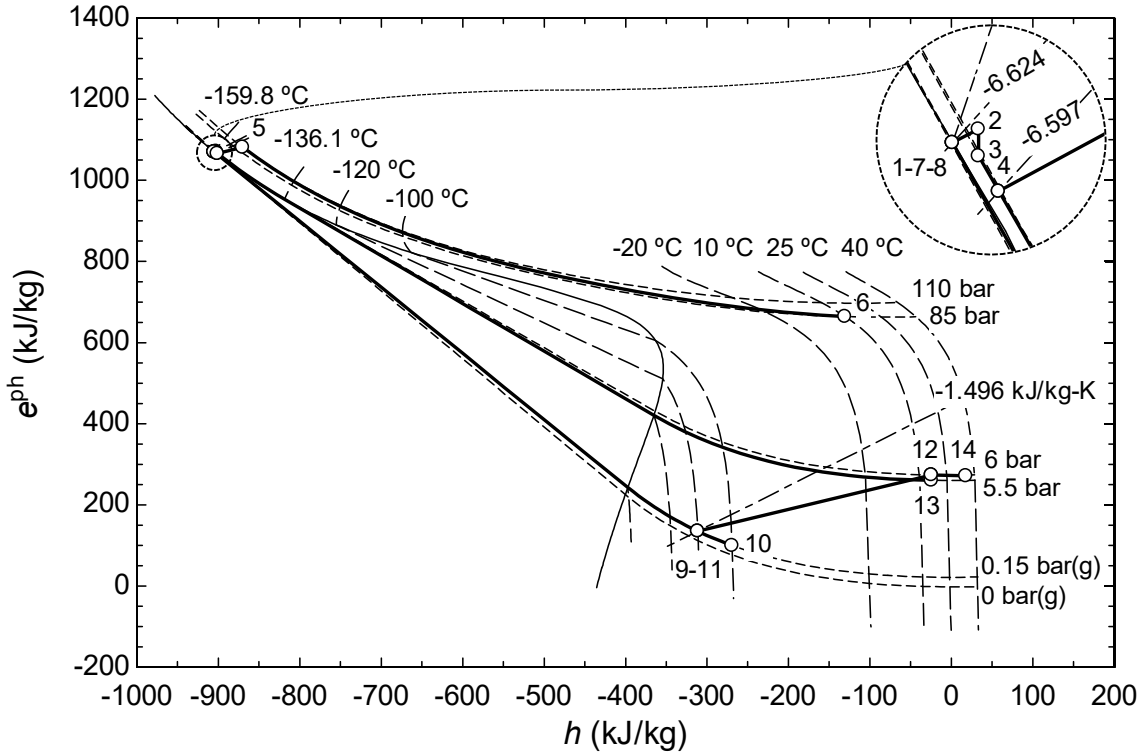

Figure 6. e^{ph}-h diagram (methane) for the seawater regasification system.

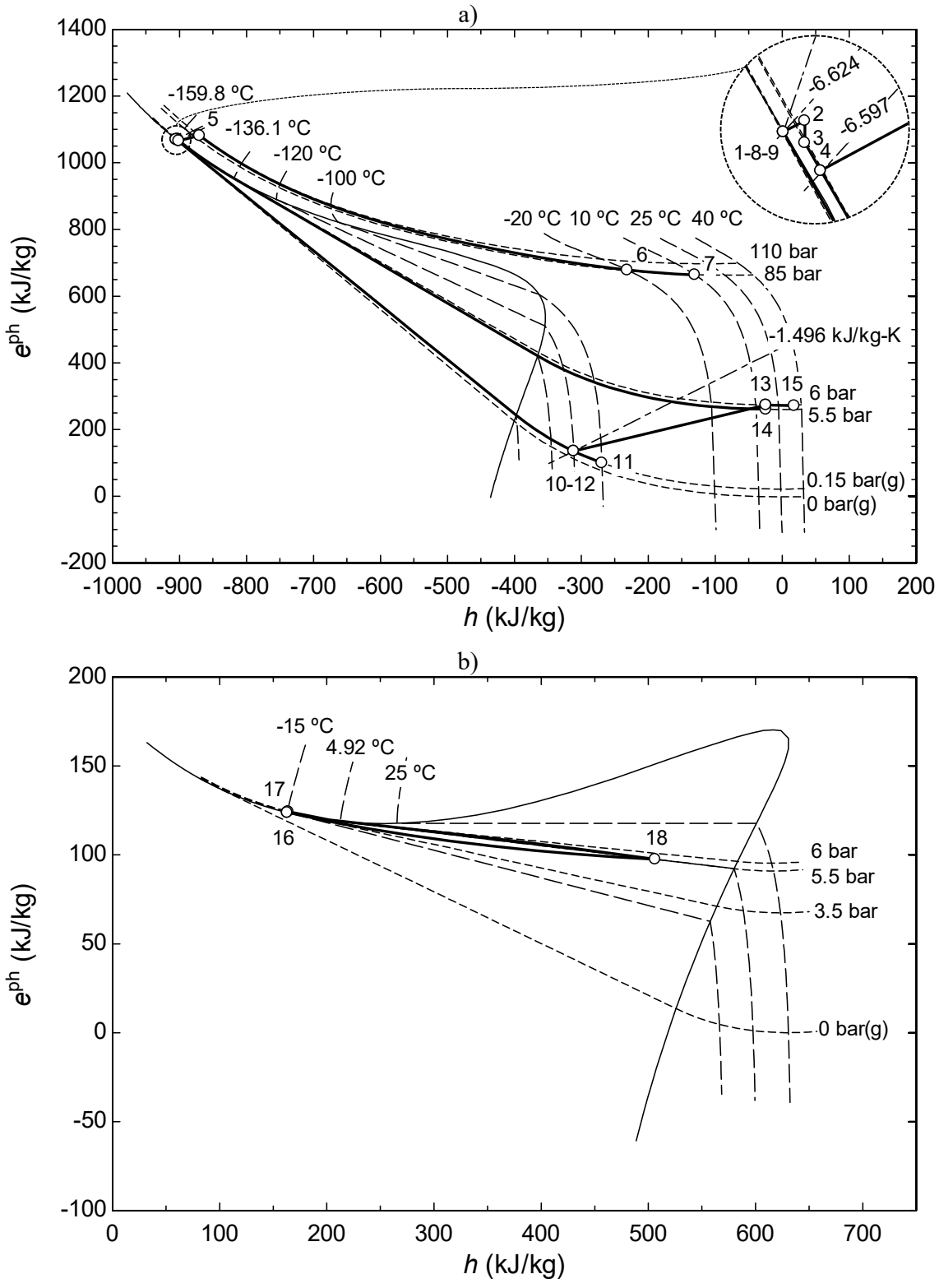

Figure 7. e^{ph}-h diagram for the open loop propane regasification system: a) methane, b) propane.

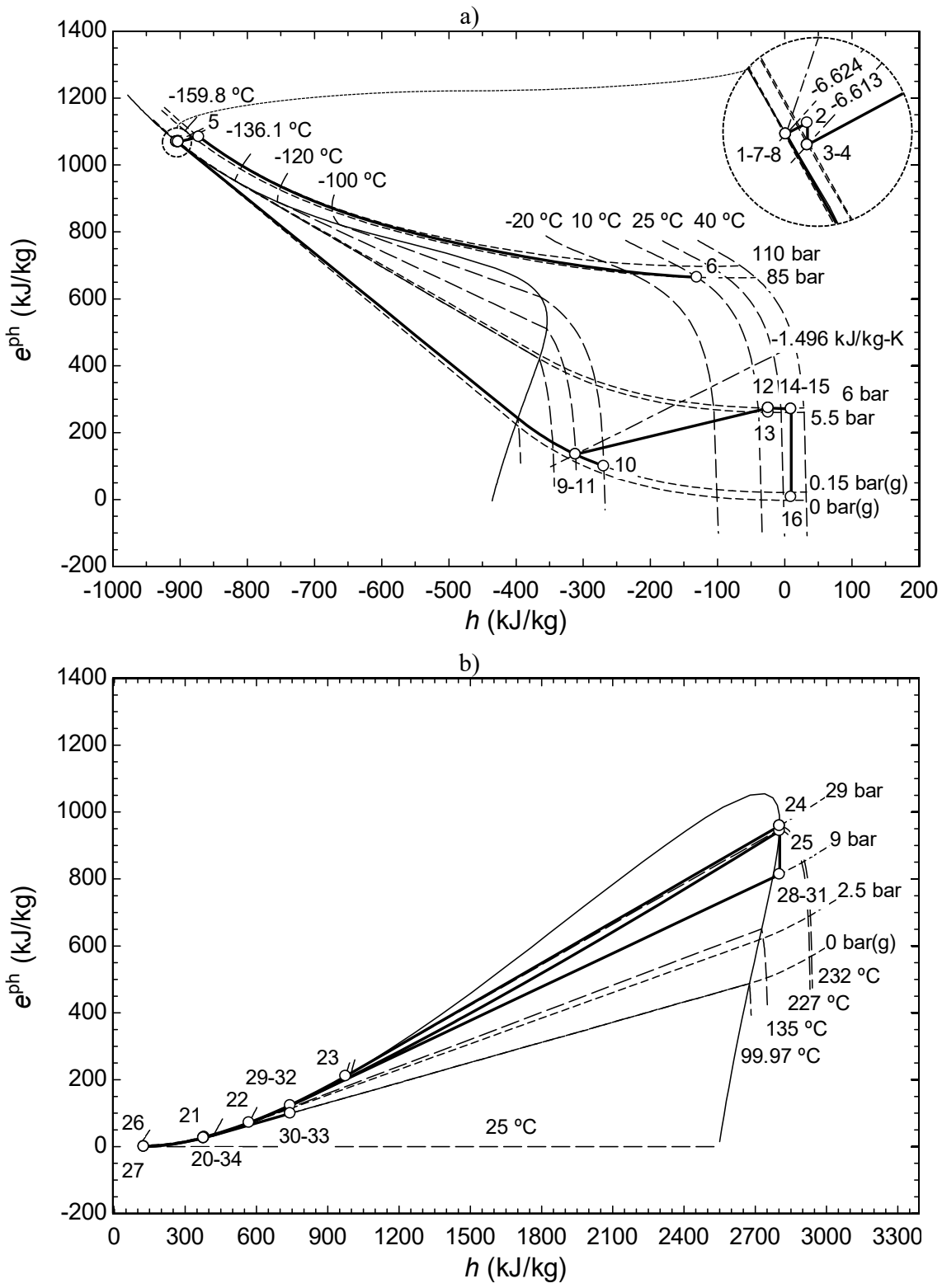

Figure 8. e^{ph}-h diagram for the closed loop water-glycol regasification system: a) methane, b) water.

Table 16 presents the relevant results of the energy analysis for each of the systems. The results obtained for the two open loop regasification systems are considerably similar. The open loop propane system demands 1.27 % more electrical power than the seawater system owing to the effect caused by the integration of the intermediate circuit, particularly the circuit pressure drops that the propane pump must manage**.** Fuel consumption in the engines, therefore, increases slightly, as does the load on the 6L50DF engine (2.33 %), the specific power consumption of the regasification system (1.61 %) and the specific energy consumption of the FSRU (1.20 %). On the other hand, the electrical input required by the FSRU in the closed loop water-glycol regasification system is reduced by 24.94 %, and the specific power consumption of the regasification system by 32.33 % in comparison with the seawater system. The reason for this is clearly illustrated in Figure 9, which shows the effect caused by the high consumption of the seawater pump due to the mass flow required to guarantee the minimum discharge temperature. However, despite reducing the electrical power of the system and, consequently, the load and fuel consumption of the engines, energy consumption per kilogram of regasified natural gas is 4.46 times above that of the seawater regasification system. This is due to the heat power required in the vaporizer which, in this case, comes from the energy released by BOG combustion in the boiler. Despite its simplicity, the seawater regasification system proves to be the most efficient from an energy perspective, closely followed by the open loop propane system.

Table 16
Main results of the energy analysis.

Parameter	**Regasification system**		
	Seawater	**Open loop propane**	**Closed loop water-glycol**
Wärtsilä 12V50DF load (%)	80.00	80.00	68.77
Wärtsilä 6L50DF load (%)	23.22	25.55	-
Electric power consumption (kW)	9921.61	10 047.44	7447.56
b_{RS} (kJ/kg)	63.47	64.49	42.95
b_{FSRU} (kJ/kg)	227.33	230.05	1013.47

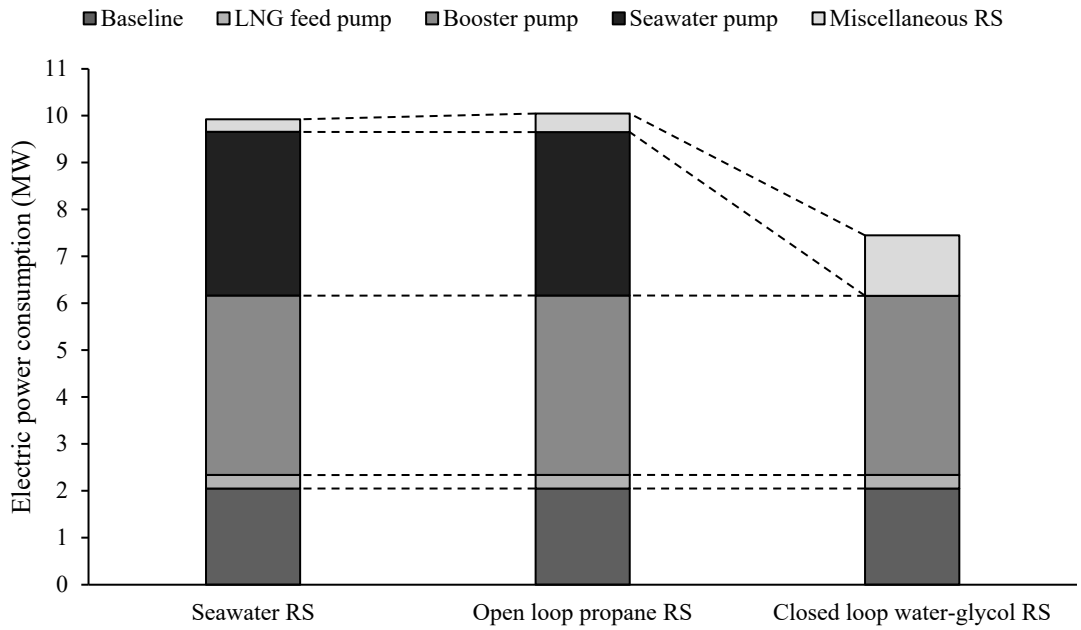

Figure 9. Electric power consumption for each regasification system.

In reference to the exergy analysis, Figure 6, Figure 7a and Figure 8a illustrate the effect caused by the feed and booster pumps in the transformation of LNG thermal exergy into mechanical one. While in the storage tank (state 1, Figure 6, Figure 7a and Figure 8a), the thermal component of exergy clearly predominates, at the inlet of the vaporizer (state 5, Figure 6, Figure 7a and Figure 8a) it is the mechanical component that renders around 60 %. Subsequently, practically all the thermal exergy contained in the LNG is lost in the vaporizer, besides the mechanical exergy destroyed due to pressure loss. Table 17 and Table 18 contain the results of the exergy provided, the exergy destroyed and the exergy efficiency for the regasification systems and the FSRU, respectively. Similar to the energy analysis, the seawater regasification system was found to be most efficient, closely followed by the open loop propane system. Table 19, Table 20 and Table 21 display the exergy destroyed and exergy efficiency per component for each regasification system.

Table 17
Main results of the exergy analysis for the regasification systems.

Parameter	**Regasification system**		
	Seawater	**Open loop propane**	**Closed loop water-glycol**
Exergy supplied (kW)	123 431.28	123 550.97	215 748.41
Exergy destruction (kW)	48 211.78	48 335.05	144 224.23
Exergy efficiency (%)	60.94	60.88	33.15

Table 18
Main results of the exergy analysis for the FSRU with the regasification systems.

Parameter	Regasification system		
	Seawater	Open loop propane	Closed loop water-glycol
Exergy supplied (kW)	142 666.38	142 987.28	235 594.90
Exergy destruction (kW)	71 330.26	71 335.99	164 296.41
Exergy efficiency (%)	50.00	49.89	30.26

Table 19
Exergy destruction and exergy efficiency by component of the seawater regasification system. In parentheses the exergy efficiency of the subsystems.

Component	Exergy destruction (irreversibilities)		Exergy efficiency
	(kW)	(%)	(%)
LNG feed pump	135.76	0.28	47.53
Recondenser / LNG inlet valve / BOG inlet valve	139.53 / 242.38 / 3.05	0.29 / 0.50 / 0.01	57.01 (32.10)
Booster pump	1739.70	3.61	49.49
Vaporizer	45 166.09	93.68	2.71
Mixer	21.71	0.05	52.66
LD compressor	109.31	0.23	48.35
Seawater pump	652.17	1.35	79.25
AC/NGH	2.09	0.00	69.77
Total	48 211.78	100.00	60.94

Table 20

Exergy destruction and exergy efficiency by component of the open loop propane regasification system. In parentheses the exergy efficiency of the subsystems.

Component	**Exergy destruction (irreversibilities)**		**Exergy efficiency**
	(kW)	**(%)**	**(%)**
LNG feed pump	135.77	0.28	47.53
Recondenser / LNG inlet valve / BOG inlet valve	135.88 / 242.40 / 2.97	0.28 / 0.50 / 0.01	56.69 (31.72)
Booster pump	1739.77	3.60	49.49
Vaporizer	39 371.56	81.46	12.15
Trim heater	1439.82	2.98	10.66
Mixer	21.71	0.04	52.66
LD compressor	109.31	0.23	48.35
Propane pump	27.17	0.06	76.91
Propane evaporator	4455.30	9.22	19.54
Seawater pump	651.28	1.35	79.25
AC/NGH	2.11	0.00	69.57
Total	48 335.05	100.00	60.88

Table 21

Exergy destruction and exergy efficiency by component of the closed loop water-glycol regasification system. In parentheses the exergy efficiency of the subsystems.

Component	**Exergy destruction (irreversibilities)**		**Exergy efficiency**
	(kW)	**(%)**	**(%)**
LNG feed pump	136.04	0.09	47.53
Recondenser / LNG inlet valve / BOG inlet valve	0.00 / 242.88 / 0.00	0.00 / 0.17 / 0.00	0.00 (0.00)
Booster pump	1744.71	1.21	49.26
Vaporizer	54 714.97	37.94	17.07
Mixer	21.43	0.01	52.66
LD compressor	337.44	0.23	48.35
Water-glycol pump	20.01	0.01	80.00
Water-glycol heater / Steam control valve / Condensate control valve	21 127.33 / 470.24 / 4.52	14.65 / 0.33 / 0.00	27.21 (26.78)
Cascade tank / Steam trap	1795.54 / 82.88	1.24 / 0.06	30.65 (29.63)
Water pump	22.57	0.02	83.59
Preheater / Steam trap	780.54 / 89.24	0.54 / 0.06	67.54 (65.29)
Economizer (boiler)	2696.33	1.87	66.22
Boiler / BOG inlet valve / Steam pressure reducing valve	57 935.33 / 501.92 / 1052.70	40.17 / 0.35 / 0.73	32.92 (31.70)
Forced draft fan	36.80	0.03	80.31
AC/NGH	8.63	0.01	43.13
Drain cooler (condenser)	402.17	0.28	23.75
Total	144 224.23	100.00	33.15

A simplified Grassmann diagram was drawn up for each regasification system in order to clearly and concisely reflect the exergy sources and the main exergy destroying components in the FSRU. In the case of the seawater regasification system (Figure 10), the variation in natural gas thermal exergy represents 81.57 % of the supplied exergy, while the chemical exergy released in the combustion process of DF engines only reaches

the 18.43 %. Moreover, most of the exergy destruction occurs in the regasification system, especially in the vaporizer, accounting for 63.32 % of the exergy destroyed in the FSRU. In the open loop propane regasification system (Figure 11), whose diagram is similar to that of the previous system, the exergy destroyed is primarily associated with two components: the vaporizer (54.96 %) and the propane evaporator (6.23 %). Lastly, in the closed loop water-glycol regasification system (Figure 12), natural gas thermal exergy variation represents 50.19 %, while 49.71 % of the remaining exergy is provided by the boiler and DF engine combustion processes. The DF engine only reaches 8.10 %, while the boiler accounts for 41.61 %. The exergy provided by air (0.6 %) is higher than that of the DO (0.4 %). This is attributable to two factors: high air flow and a composition different from that of the environment. On the other hand, the system destroys 69.74 % of the exergy provided. Within the exergy destroyed, the regasification system irreversibilities reached 87.78 %. The primary exergy destroying components for this system are the boiler (35.26 %), the vaporizer (33.30 %) and the water-glycol heater (12.86 %).

Unlike the open loop regasification systems under study, the closed loop water-glycol system destroys not only the exergy linked to LNG low temperature, but also that associated to the high temperature deriving from the boiler combustion process. The latter causes the exergy destroyed in the closed loop water-glycol regasification system to be three times that of open loop systems. Although the open loop systems studied prove to be more efficient, in terms of exergy exploitation, the closed loop water-glycol system has greater potential since, as well as LNG cold exergy, it also has a high temperature heat source.

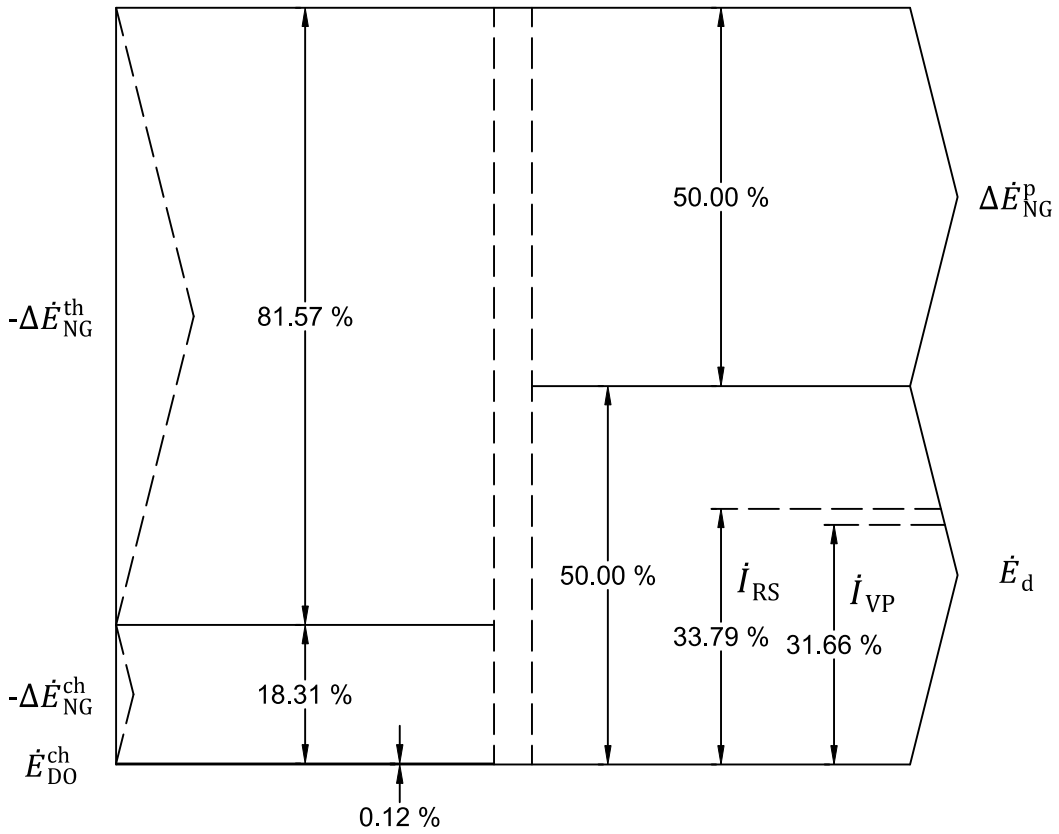

Figure 10. Grassmann diagram for the FSRU with the seawater RS.

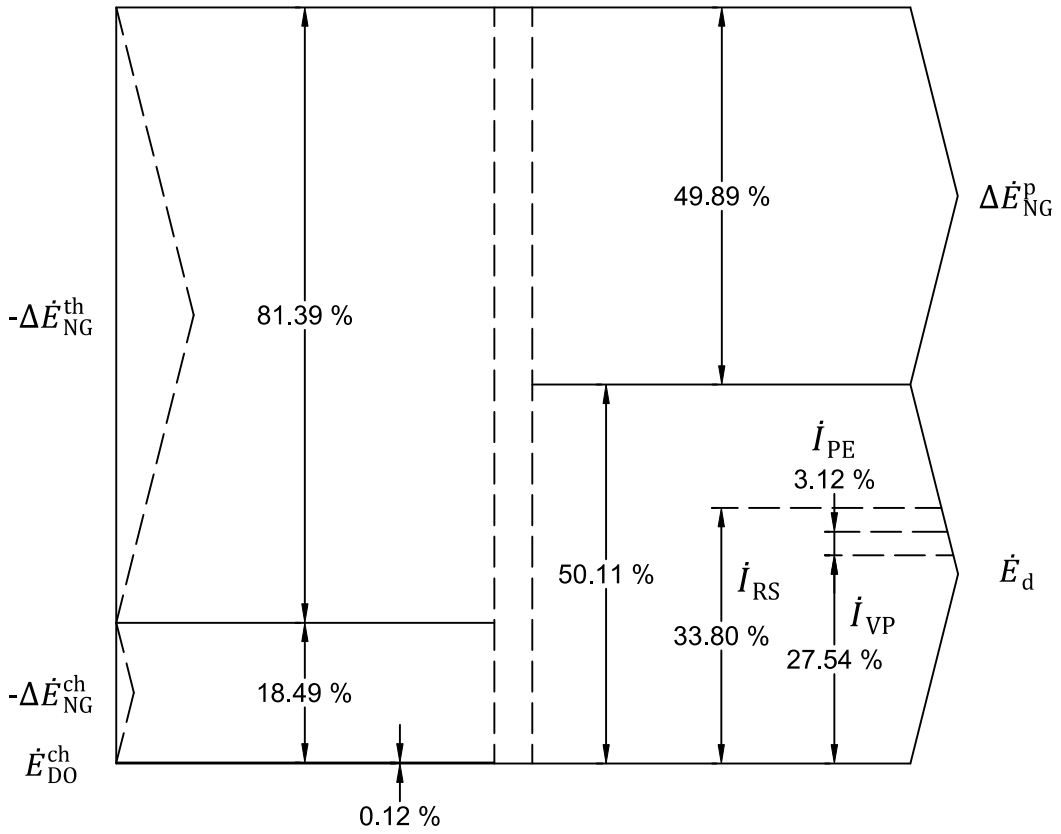

Figure 11. Grassmann diagram for the FSRU with the open loop propane RS.

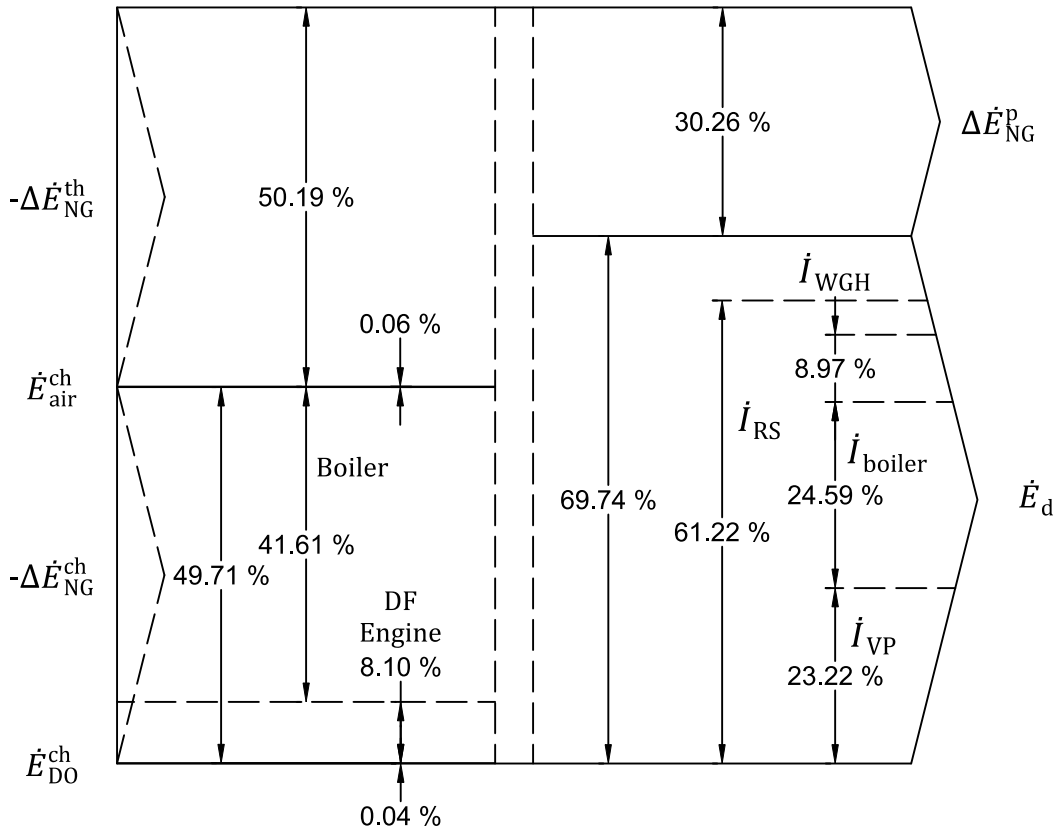

Figure 12. Grassmann diagram for the FSRU with the closed loop water-glycol RS.

4.1.1 Effect of boil off rate

Regarding the design conditions of the model FSRU, the BOR is one of the most important parameters which in recent years has been significantly reduced in LNG carriers due to the installation of better insulated storage tanks. Figure 13a and Figure 13b depict the effect of BOR reduction on the mass flows of forced BOG and condensed BOG for the three regasification systems studied. As the BOR decreases in open loop regasification systems, the condensed BOG in the recondenser reduces until the minimum BOR point is reached. In this condition, the excess BOG is zero and the tanks generate enough BOG to supply the natural gas demand without using the forcing vaporizer. The minimum BOR points for the seawater and propane open loop systems are 0.1236 and 0.1243 %, respectively. This value is slightly higher in the open loop propane system due to the power consumption of the propane pump. The reduction of the BOR in the case of the closed loop water-glycol system only contributes to an increase of the forced BOG in the forcing vaporizer as the minimum point is above 0.15 %.

Figure 14a and Figure 14b show the effect of BOR on FSRU specific energy consumption and exergy efficiency for the regasification systems analysed. In the open loop systems, the specific energy consumption decreases until the minimum BOR point is reached. The obtained values of specific energy consumption in this condition for the seawater and propane open loop systems are 225.48 and 228.37 kJ/kg, respectively. A BOR lower than the minimum BOR point does not influence the specific energy consumption. This is justified for two reasons: the electrical power of the regasification system remains constant in the absence of excess BOG and the engines economisers are sufficient to supply the demand of the auxiliary steam system (condition assumed in section 2.3). However, the behaviour of the exergy efficiency is different. The maximum exergy efficiency in the seawater system is reached at the minimum BOR point, while the efficiency in the open loop propane system decreases slightly until the minimum BOR point is reached. This unequal behaviour is justified by the negative effect of the pressure drop in the intermediate propane circuit. Below the minimum BOR point, the exergy efficiency decreases in all regasification systems because of the cold exergy that is destroyed in the forcing vaporizer.

Figure 15a and Figure 15b depict the effect of LNG storage capacity in the range of 160 000-180 000 m^3 on the minimum BOR point. An increase in storage capacity increases the BOG generation in the tanks, therefore, the minimum BOR point decreases. For a storage capacity of 180 000 m^3, the minimum BOR point of the seawater and propane open loop systems decreases to 0.1167 and 0.1174 %, respectively. This represents a reduction for both systems of 5.58 and 5.55 % compared to the values obtained with the reference storage capacity. In contrast, the minimum BOR point for the closed loop water-glycol system is more than three times higher than for the open loop systems and is well above the design BOR of the current membrane tanks.

a)

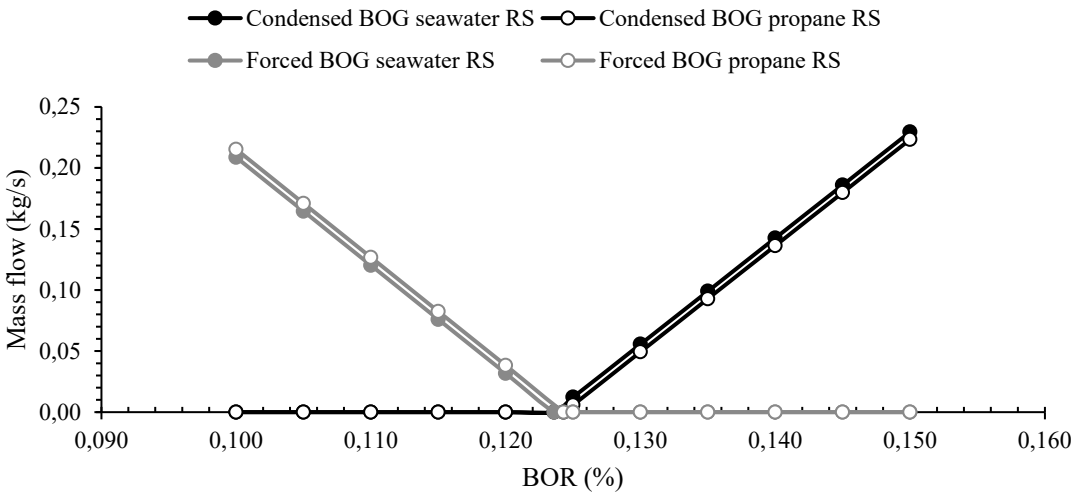

b)

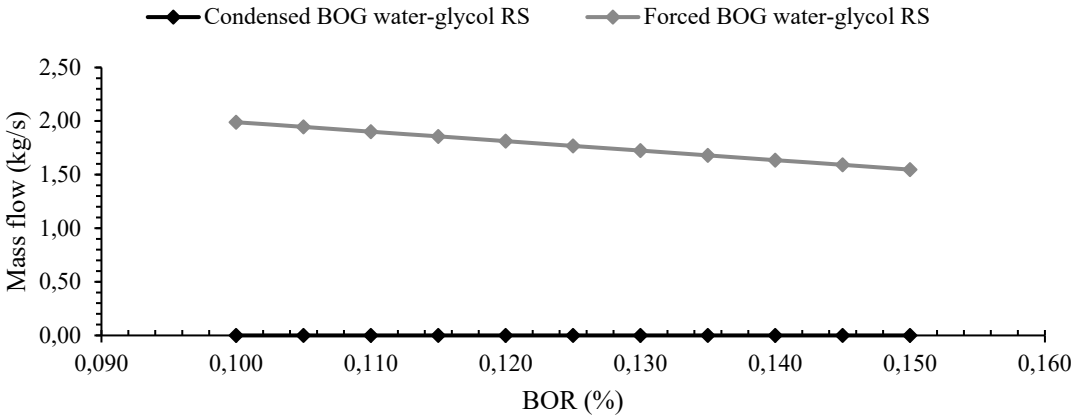

Figure 13. BOR effect on the forced and condensed BOG: a) open loop RS, b) closed loop water-glycol RS.

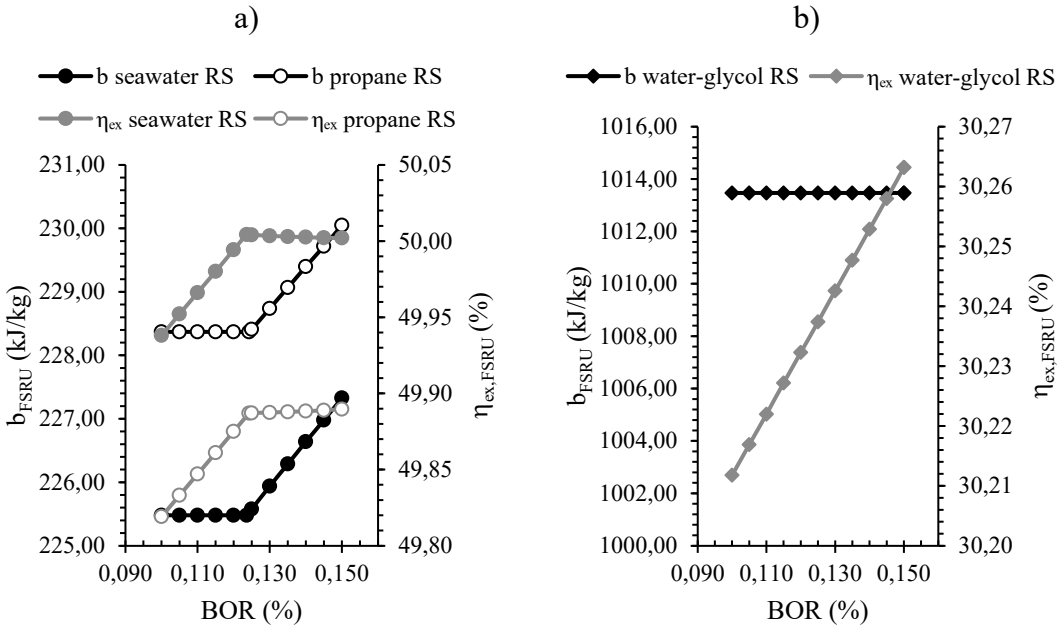

Figure 14. BOR effect on the specific energy consumption and exergy efficiency of the FSRU: a) open loop RS, b) closed loop water-glycol RS.

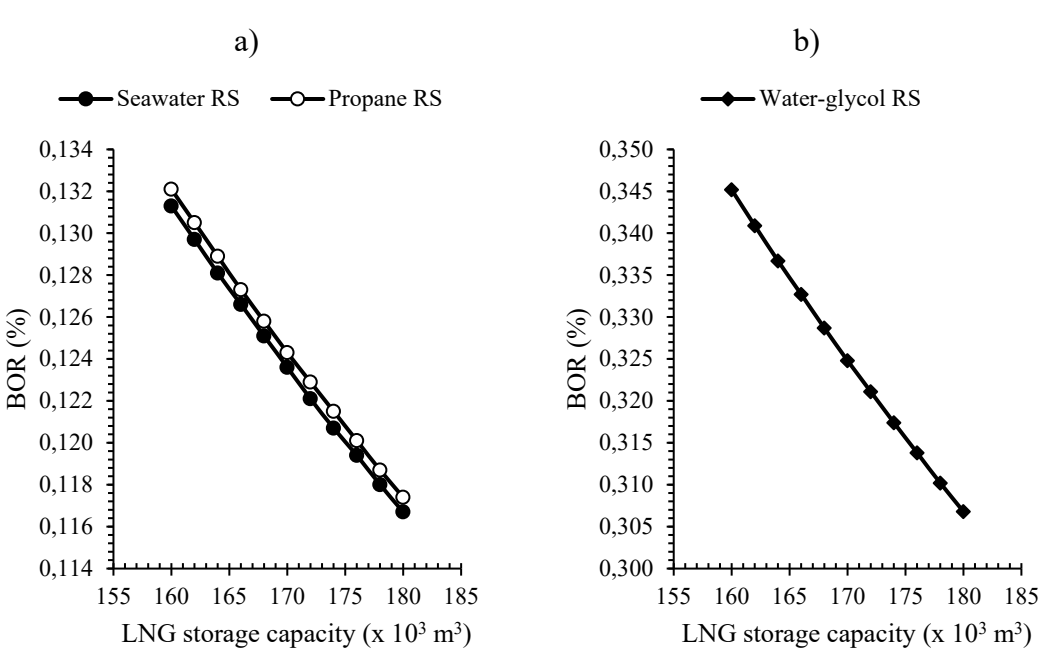

Figure 15. Effect of the LNG storage capacity on the minimum BOR point: a) open loop RS, b) closed loop water-glycol RS.

4.2 Economics

The main characteristics of heat exchangers designed with the EDR program are presented in Table 22. Titanium was the chosen material for the heat exchangers that use seawater, whilst low-carbon stainless steel (SS316L) was selected for all others. Alongside the choice of material, the exchanger type is particularly important in terms of the total capital cost of the modules; plate heat exchangers allow for a more compact design compared to shell and tube heat exchangers. Table 23 illustrates the economic outcome of the regasification modules obtained with the APEA program. The total capital investment assessment suggests that the closed loop regasification system with water-glycol, without taking into account the steam installation, is the most economical, approximately 40 % less expensive than those open loop systems studied. This difference can be attributed to the fact that the material of construction of all the heat exchangers (water-glycol heaters and vaporizers) of this system is SS316L. Therefore, the heat exchangers represent 26.02 % of the total cost of the equipment, while in the installed cost the value increases to 33 %. However, in the open loop regasification systems analysed, the effect of titanium in the installed cost of the exchangers becomes extremely important. The factor between the installed cost and the cost of the equipment of these heat exchangers is in the range of 2.70 (propane evaporators) to 4.25 (seawater vaporizers). Thus, the seawater system vaporizers represent 36.34 % of the total cost of the equipment, but if the cost installed is observed, the value is 65.76 %. In the propane system, despite having more components, the total capital cost is reduced by 2.67 % compared to the seawater system. This is due to the propane evaporators (titanium plate exchangers) and the vaporizer built in SS316L.

Moreover, Figure 16a and Figure 16b depict the cost rate for each of the regasification systems based on the price of LNG. Overall, the open loop propane system is most cost-effective for an LNG price of between 1.32 and 11 USD/MMBtu. This is justified by a lower total capital cost than the seawater system and a fairly similar efficiency. In contrast, high BOG consumption in the boiler of the closed loop water-glycol regasification system clearly disadvantages its cost rate with the increasing cost of LNG. Results obtained illustrate that the closed loop system analysed is economically viable for an LNG price of under 1.32 USD/MMBtu. However, this value, obtained from the intersection point between the open loop propane system and the closed loop water-glycol system in Figure 16b, is affected by the volatile price of DO or the interest rate considered in the project.

Table 22
Main specifications of heat exchangers obtained from the EDR.

Modules	Heat exchanger	Parameter	Value
Seawater	Vaporizer	TEMA type	NJN
		Tube external diameter (mm)	19.03
		Tube pitch (mm)	23.81
		Tube pattern (°)	45
		Material	Titanium
		Shell internal diameter (mm)	975
		Tube length (mm)	12 900
		Baffle spacing (mm)	590
		Number of baffles	16
		Number of tubes / passes	785 / 1
Propane	Vaporizer	TEMA type	NEN
		Tube external diameter (mm)	19.03
		Tube pitch (mm)	23.81
		Tube pattern (°)	30
		Material	Titanium
		Shell internal diameter (mm)	900
		Tube length (mm)	9550
		Baffle spacing (mm)	590
		Number of baffles	13
		Number of tubes / passes	928 / 1
	Trim heater	TEMA type	NEN
		Tube external diameter (mm)	19.03
		Tube pitch (mm)	23.81
		Tube pattern (°)	45
		Material	316L
		Shell internal diameter (mm)	1125
		Tube length (mm)	5700
		Baffle spacing (mm)	520
		Number of baffles	9
		Number of tubes / passes	1118 / 3

Table 22
Main specifications of heat exchangers obtained from the EDR.

Modules	Heat exchanger	Parameter	Value
	Propane evaporator	Type	PHE
		Chevron angle (°)	45
		Material	Titanium
		Heat transfer area (m^2)	988.96
		Number of plates	357
Water-glycol	Vaporizer	TEMA type	NEU
		Tube external diameter (mm)	19.03
		Tube pitch (mm)	23.81
		Tube pattern (°)	30
		Material	316L
		Shell internal diameter (mm)	1025
		Tube length (mm)	5 850
		Baffle spacing (mm)	520
		Number of baffles	10
		Number of tubes / passes	1166 / 4
	Water-glycol heater	TEMA type	NEN
		Tube external diameter (mm)	19.03
		Tube pitch (mm)	23.81
		Tube pattern (°)	30
		Material	316L
		Shell internal diameter (mm)	1425
		Tube length (mm)	6000
		Baffle spacing (mm)	570
		Number of baffles	8
		Number of tubes / passes	2823 / 1

Table 23
Economic results obtained from the APEA. Centrifugal pump (CP), shell and tube heat exchanger (S&T) and plate heat exchanger (PHE).

Modules	Equipment	n. º	Type / Material	Equip. cost (USD)	Installed cost (USD)	Total capital cost (USD)
Seawater	Booster pump	6	CP / SS304	8 322 000	10 483 800	49 363 900
	Vaporizer	6	S&T / Titanium	4 751 400	20 131 400	
Propane	Booster pump	6	CP / SS304	8 322 000	10 483 800	48 072 400
	Vaporizer	3	S&T / SS316L	1 051 500	2 244 300	
	Trim heater	3	S&T / Titanium	2 006 700	7 775 300	
	Propane pump	3	CP / SS304	112 800	675 600	
	Propane evaporator	9	PHE / Titanium	2 597 400	7 027 600	
Water-glycol	Booster pump	6	CP / SS304	8 322 000	10 483 800	29 687 800
	Vaporizer	3	S&T / SS316L	983 400	2 147 200	
	Water-glycol pump	3	CP / SS304	87 300	562 200	
	Water-glycol heater	3	S&T / SS316L	1 980 000	3 196 100	

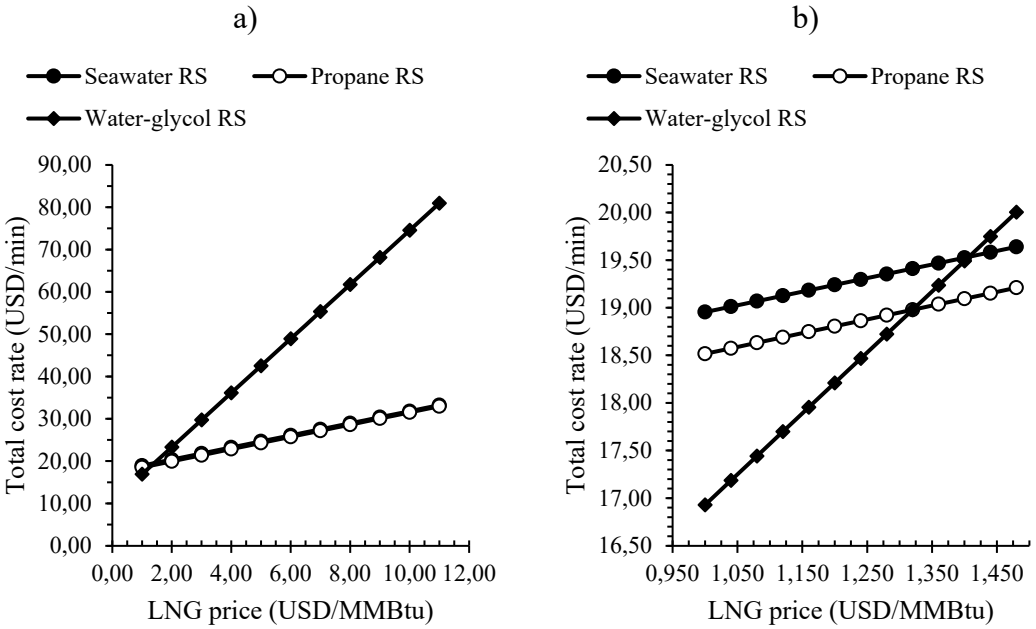

Figure 16. Total cost rate of the regasification systems as a function of the LNG price: a) LNG price range 1-11 USD/MMBtu, b) LNG price range 1-1.5 USD/MMBtu.

4.3 Effect of DO price and interest rate

Figure 17a and Figure 17b depict respectively the total cost rate and the LNG price of the intersection point as a function of the DO price and the interest rate. The increase in the price of DO benefits the regasification system with the lowest electrical power consumption, i.e., the closed loop water-glycol system. Therefore, if the DO price increases to a value of 700 USD/t, the closed loop system becomes more economical for an LNG price below 1.325 USD/MMBtu. Despite a 40 % increase in the DO price compared to the reference case, this represents a 0.36 and 0.28 % increase respectively in the LNG price and total cost rate; the explanation lies in the fact that DO is not the main fuel for DF engines. However, the effect of the interest rate on these parameters is more significant. Decreasing the interest rate from 12 to 10 % (reduction of less than 17 %) implies respectively a reduction of 9.96 and 9.98 % in the LNG price and total cost rate. Furthermore, the relationship between interest and the LNG price or total cost rate is almost linear in a typical range of 4-14 % of the former. Therefore, the reduction in the interest rate benefits open loop regasification systems which, despite having a higher capital investment cost, significantly reduce the consumption of natural gas in the FSRU.

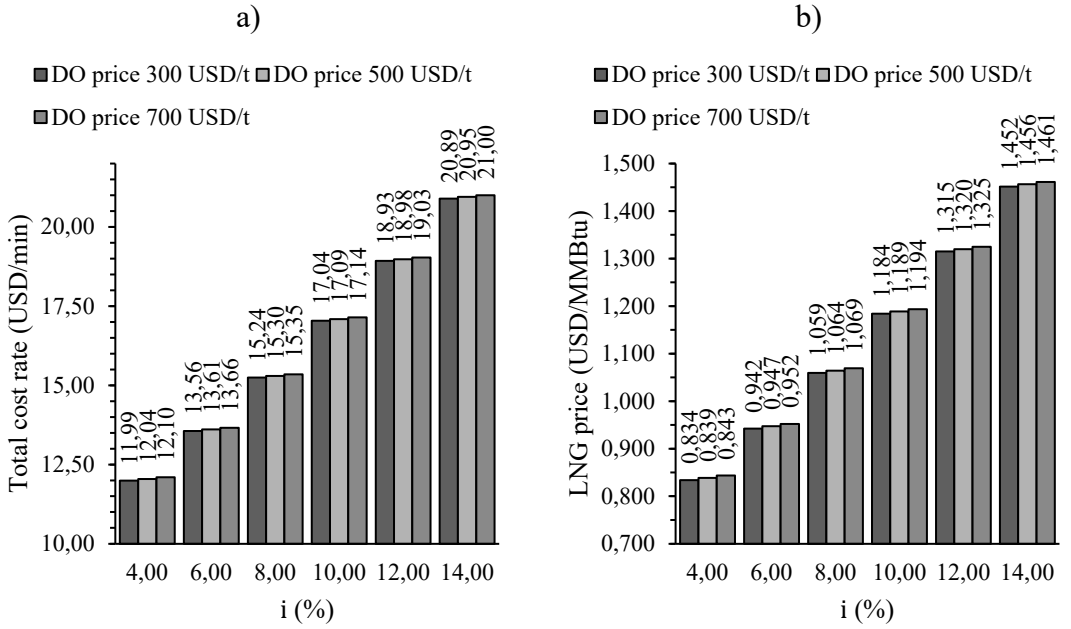

Figure 17. Effect of the DO price and interest rate on the intersection point: a) Total cost rate of the intersection point, b) LNG price of the intersection point.

5 Conclusions

In this study, an energy, exergy and economic analysis is elaborated for the assessment of regasification systems in FSRUs. The analysis applies to three common regasification systems: seawater system, open loop propane system, and closed loop water-glycol system. The main conclusions obtained from the analysis are as follows:

- The energy analysis demonstrates that the seawater regasification system is most efficient, since the specific energy consumption is less for the same mass flow of regasified natural gas than the other systems. The open loop propane system compares similarly to the preceding. By contrast, despite the low power consumption, the closed loop water-glycol system requires four times more energy per kilogram of regasified natural gas than the seawater system.
- The exergy study indicates that natural gas regasification is clearly destructive of exergy, hence the components of physical exergy (thermal and mechanical exergy) require further analysis in order to develop an equation that allows evaluation of the regasification system exergy efficiency. From this standpoint, a regasification system converts the natural gas thermal exergy into mechanical exergy at the expense of pump and compressor consumption, and of the contribution of exergy from some combustion process, the latter being applicable to systems with closed loop operation. Based on this definition, the exergy efficiency of the seawater regasification system is 60.94 %, while that of the open loop propane system results to be 60.88 % and that of the closed loop glycol water system 33.15 %.
- Pursuant to the regasification system exergy efficiency definition, another can be developed for the exergy efficiency of the FSRU as a whole. Here, the exergy of the DF engine combustion process is included instead of the power consumed by pumps and compressors, and those flows that evolve up to conditions of reference or initial state are assumed as destroyed exergy. On the basis of this definition, the exergy efficiency of the seawater regasification system is 50.00 %, while that of the open loop propane system is 49.89 %, and that of the closed loop glycol water system 30.26 %.
- In the analysed open loop regasification systems, the vaporizer, which is related to the LNG cold exergy, is the component where the greatest irreversibilities occur. However, exergy destruction in the boiler combustion process of the closed loop water-glycol system exceeds that of the LNG vaporizer.
- From an exergy-exploitation perspective, the closed loop water-glycol regasification system has the greatest potential since, in addition to the cold exergy of the LNG, it also benefits from the exergy from the boiler combustion process. In effect, higher capacity residual energy recovery systems could be implemented than in open loop regasification systems.

- The economic analysis, taking the total capital cost of the regasification modules, fuel prices, and maintenance and operation associated costs into account, reveals that the open loop propane regasification system is most cost-effective for an LNG price of between 1.32 and 11 USD/MMBtu. For an LNG price under 1.32 USD/MMBtu, the closed loop regasification system obtains the lowest cost rate, but the assessment does not allow for expenses associated with the steam plant.

The energy, exergy and economic analysis carried out in the present paper can be implemented when evaluating regasification systems that may or may not include residual energy recovery systems. The vast amount of exergy destroyed in current regasification systems installed in FSRUs has been displayed, and hence the need to implement new, more efficient systems which allow exploitation of the regasification process exergy in order to reduce fuel consumption, emissions and the cost rate.

References

[1] S. Mokhatab, W.A. Poe, J.Y. Mak, Handbook of natural gas transmission and processing: Principles and practices, 2018. https://doi.org/10.1016/C2017-0-03889-2.

[2] S. Mokhatab, J.Y. Mak, J. V. Valappil, D.A. Wood, Handbook of Liquefied Natural Gas, Elsevier, 2014. https://doi.org/10.1016/C2011-0-07476-8.

[3] J. Norrgård, LNG terminals – land-based vs. floating storage and regasification technology, Wärtsilä Tech. J. (2018). https://www.wartsila.com/twentyfour7/in-detail/lng-terminals-land-based-vs-floating-storage-and-regasification-technology.

[4] G. Tusiani, Michael D; Shearer, LNG: A Nontechnical Guide, PennWell, 2007.

[5] IGU, 2020 World LNG Report, 2020.

[6] Excelerate Energy, Floating Storage Regasification Unit (FSRU) - Excelerate Energy, (2020). https://excelerateenergy.com/fsru/ (accessed July 2, 2020).

[7] U.S. Coast Guard; engineering-environmental Management, Neptune LNG Deepwater Port License Application: Environmental Impact Statement, 2006.

[8] B. Songhurst, The Outlook for Floating Storage and Regasification Units (FSRUs), Oxford, United Kingdom, 2017. https://doi.org/https://doi.org/10.26889/9781784670894.

[9] B. Songhurst, Floating LNG update, Oxford, United Kingdom, 2019. https://doi.org/10.26889/9781784671440.

[10] K.O. Ulstein, P.H. Madsen, Wärtsilä Corporation, Grasping the potential, (2020). https://www.wartsila.com/insights/article/gasping-the-potential (accessed June 3, 2021).

[11] Mitsui O.S.K. Lines, MOL and DSME Obtain AIP for Design of FSRU “Cryo-Powered Regas” System - Development of New Technology to Reduce Environmental Impact -, (2020). https://www.mol.co.jp/en/pr/2020/20016.html.

[12] T. He, Z.R. Chong, J. Zheng, Y. Ju, P. Linga, LNG cold energy utilization: Prospects and challenges, Energy. 170 (2019) 557–568. https://doi.org/10.1016/j.energy.2018.12.170.

[13] B.B. Kanbur, L. Xiang, S. Dubey, F.H. Choo, F. Duan, Cold utilization systems of LNG: A review, Renew. Sustain. Energy Rev. 79 (2017) 1171–1188. https://doi.org/10.1016/j.rser.2017.05.161.

[14] E. Baldasso, M.E. Mondejar, S. Mazzoni, A. Romagnoli, F. Haglind, Potential of liquefied natural gas cold energy recovery on board ships, J. Clean. Prod. 271 (2020) 122519. https://doi.org/10.1016/j.jclepro.2020.122519.

[15] E.L. Tsougranis, D. Wu, A feasibility study of Organic Rankine Cycle (ORC) power generation using thermal and cryogenic waste energy on board an LNG passenger vessel, Int. J. Energy Res. 42 (2018) 3121–3142. https://doi.org/10.1002/er.4047.

[16] F. Han, Z. Wang, Y. Ji, W. Li, B. Sundén, Energy analysis and multi-objective optimization of waste heat and cold energy recovery process in LNG-fueled vessels based on a triple organic Rankine cycle, Energy Convers. Manag. 195 (2019) 561–572. https://doi.org/10.1016/j.enconman.2019.05.040.

[17] J. Koo, S.R. Oh, Y.U. Choi, J.H. Jung, K. Park, Optimization of an organic Rankine cycle system for an LNG-powered ship, Energies. 12 (2019). https://doi.org/10.3390/en12101933.

[18] Z. Tian, Y. Yue, B. Gu, W. Gao, Y. Zhang, Thermo-economic analysis and optimization of a combined Organic Rankine Cycle (ORC) system with LNG cold energy and waste heat recovery of dual-fuel marine engine, Int. J. Energy Res. 44 (2020) 9974–9994. https://doi.org/10.1002/er.5529.

[19] L. Yoon-Ho, LNG-FSRU cold energy recovery regasification using a zeotropic mixture of ethane and propane, Energy. 173 (2019) 857–869. https://doi.org/10.1016/j.energy.2019.02.111.

[20] S. Yao, H. Liu, L. Tang, Y. Ye, L. Zhang, Thermodynamic analysis and optimization for cold energy utilization based on low temperature rankine cycle of LNG-FSRU regasification system, Int. J. Simul. Syst. Sci. Technol. 17 (2016) 35.1-35.9. https://doi.org/10.5013/IJSSST.a.17.30.35.

[21] S. Lee, B.C. Choi, Thermodynamic assessment of integrated heat recovery system combining exhaust-gas heat and cold energy for LNG regasification process in FSRU vessel, J. Mech. Sci. Technol. 30 (2016) 1389–1398. https://doi.org/10.1007/s12206-016-0246-y.

[22] L. Yoon-Ho, Thermo-economic analysis of a novel regasification system with liquefied-natural-gas cold-energy, Int. J. Refrig. 101 (2019) 218–229. https://doi.org/10.1016/j.ijrefrig.2019.03.022.

[23] S. Yao, L. Xu, L. Tang, New cold-level utilization scheme for cascade three-level Rankine cycle using the cold energy of liquefied natural gas, Therm. Sci. 2018 (2018) 3865–3875. https://doi.org/10.2298/TSCI171012239Y.

[24] Gaztransport & Technigaz, GTT | Mark III systems, (2020). https://www.gtt.fr/en/technologies/markiii-systems (accessed September 5, 2020).

[25] Samsung Heavy Industries, S-REGAS Regasification System (Brochure), (2014).

[26] P.H.S. Madsen, D. Karsten, R. Strande, Intermediate fluid vaporizers for LNG re-gasification vessels, SRVs and FSRU's, Proc. Annu. Offshore Technol. Conf. 3 (2010) 2185–2198. https://doi.org/10.4043/20809-ms.

[27] Y. Eum, S. Kim, K. Doh, M. Ha, Eco-friendly LNG SRV: Completion of the regas trial, Int. Gas Res. Conf. Proc. 4 (2011) 2791–2803.

[28] J. Szargut, Exergy method: technical and ecological applications, WIT Press, 2005.

[29] S.A. Klein, Engineering Equation Solver (EES), (2015).

[30] S. Kakaç, H. Liu, A. Pramuanjaroenkij, Heat Exchangers: Selection, Rating, and Thermal Design, Third Edition, 2012. https://books.google.com/books?hl=en&lr=&id=sJXpvP6xLZsC&pgis=1.

[31] M.H. Sharqawy, J.H. Lienhard V, S.M. Zubair, Erratum to Thermophysical properties of seawater: A review of existing correlations and data, Desalin. Water Treat. 29 (2011) 355–355. https://doi.org/10.5004/dwt.2011.2947.

[32] K.G. Nayar, M.H. Sharqawy, L.D. Banchik, J.H. Lienhard, Thermophysical properties of seawater: A review and new correlations that include pressure dependence, Desalination. 390 (2016) 1–24. https://doi.org/10.1016/j.desal.2016.02.024.

[33] J. Romero Gómez, M. Romero Gómez, J. Lopez Bernal, A. Baaliña Insua, Analysis and efficiency enhancement of a boil-off gas reliquefaction system with cascade cycle on board LNG carriers, Energy Convers. Manag. 94 (2015) 261–274. https://doi.org/10.1016/j.enconman.2015.01.074.

[34] C. Migliore, C. Tubilleja, V. Vesovic, Weathering prediction model for stored liquefied natural gas (LNG), J. Nat. Gas Sci. Eng. 26 (2015) 570–580. https://doi.org/10.1016/j.jngse.2015.06.056.

[35] C.A. Frangopoulos, Exergy, Energy System Analysis and Optimization Volume - I: Exergy and Thermodynamic Analysis, EOLSS Publications, Oxford, United Kingdom, 2009.

[36] A. Bejan, G. Tsatsaronis, M. Moran, Thermal Design and Optimization, John Wiley & Sons, Ltd, 1996.

[37] Aspen Technology, Suite AspenONE, (2019).

[38] E. Querol, B. Gonzalez-Regueral, J.L. Perez-Benedito, Practical Approach to Exergy and Thermoeconomic Analyses of Industrial Processes, 2013. http://www.springer.com/series/8903.

[39] CEPCI Archives - Chemical Engineering, (2020). https://www.chemengonline.com/tag/cepci/ (accessed September 5, 2020).

[40] Ship & Bunker, World Bunker Prices - Ship & Bunker, (2020). https://shipandbunker.com/prices/ (accessed September 5, 2020).